Renewable and Sustainable Energy Reviews 38 (2014) 131–153

Contents lists available at ScienceDirect

Renewable and Sustainable Energy Reviews

journal homepage: www.elsevier.com/locate/rser

Synthesis of green fuels from biogenic waste through thermochemical route – The role of heterogeneous catalyst: A review

Pravakar Mohanty [a,b], Kamal K. Pant [a,*], Satya Narayan Naik [c], Jigisha Parikh [d], Andreas Hornung [e], J.N. Sahu [f,g,**]

[a] Department of Chemical Engineering, Indian Institute of Technology, Delhi 110016, India
[b] Sardar Patel Renewable Energy Research Institute (SPRERI), V V Nagar, Gujarat 388120, India
[c] Centre for Rural Development and Technology Indian Institute of Technology, Delhi 110016, India
[d] Department of Chemical Engineering, Sardar Vallabhbhai National Institute of Technology, Surat 395007, India
[e] School of Chemical Engineering, College of Engineering and Physical Sciences University of Birmingham, University of Birmingham, Edgbaston B15 2TT, UK
[f] Department of Chemical Engineering, Faculty of Engineering, University of Malaya, 50603 Kuala Lumpur, Malaysia
[g] Petroleum and Chemical Engineering Programme Area, Faculty of Engineering, Institut Teknologi Brunei (A Technology University), Tungku Gadong, P.O. Box 2909, Brunei Darussalam

ARTICLE INFO

Article history:
Received 8 February 2013
Received in revised form 17 April 2014
Accepted 3 May 2014
Available online 14 June 2014

Keywords:
Synthesis gas
Catalyst
Catalyst characterization
Thermochemical synthesis
Biofuels

ABSTRACT

Using gas-to-liquids (GTL) technology will expand a new horizon as resources of crude oil diminish. Fischer–Tropsch synthesis (FTS) is a part of thermo-chemical route, which is used to produce chemicals, gasoline and diesel range fuel from synthesis gas derived from different sources, including coal, oil shale, tar sands, heavy residues, biomass, or natural gases. The FTS products are predominantly linear, since purified synthesis gases are used converting into sulfur and nitrogen free products. In this review the usage of bifunctional catalysts, where major contribution of promoters likes Rh-, Ru- with different modifiers like Zr, Ga, Si, Al, B, Cr, Ce, etc. and different supports like zeolites (ZSM-5), silica and alumina have been discussed. Selective synthesis of gasoline to higher-range hydrocarbons (C_{5+}–C_{18+}) and more have been discussed in different schematic ways, by considering different heterogeneous catalyst preparation techniques using various process parameters like mole H_2/CO, CO_2/(CO+CO_2) ratios, pressures, temperatures, gas hourly space velocity and their effect on the CO% conversion. Catalytic activity and product selectivity studies with various methods of catalyst preparation technique and the characterization of different catalysts has also been discussed through this work. Different methods to modify the product distribution through thermo-chemical route by combining reaction engineering and improved catalysis synthesis techniques have been covered in this review.This may be realized through the development of new engineered catalysts tuned with careful control of mass transport effects. With new catalysts and optimal control of reactor operating conditions, the distribution of products could be tailored and/or maximized to meet market demands and thus maximize GTL plant operations.

Contents

* Corresponding author. Tel.: +91 1126596177; fax: +91 1126581120.
** Corresponding author at: Department of Chemical Engineering, Faculty of Engineering, University of Malaya, 50603 Kuala Lumpur, Malaysia.
E-mail addresses: pravakar.mohanty@gmail.com (P. Mohanty), kkpant@chemical.iitd.ac.in (K.K. Pant), jay_sahu@yahoo.co.in (J.N. Sahu).

http://dx.doi.org/10.1016/j.rser.2014.05.011
1364-0321/

1. Introduction

The demand for energy is increasing globally due to the rapid outgrowth of population, urbanization and industrial development. The socio-environmental concerns associated with conventional fossil fuels such as elevating fuel prices, pollution and global warming are encouraging a move towards renewable resources. Since the discovery of Fischer–Tropsch synthesis (FTS) in the late 1920s by two German scientists named F. Fischer and H. Tropsch, numerous review papers, books and reports have addressed FTS mechanisms and kinetics [1,2]. As catalysts play a vital part of any industrial FTS process. Catalysts containing iron are employed for the production of lighter hydrocarbons, paraffins and olefins during the FTS process at high temperatures. They are essentially synthesized by the conversion of syngas with low H_2/CO ratio between 1 and 2. A recent development of FTS involves syngas with high H_2/CO ratio, which is produced from natural gas [3,4]. In history, the energy deficit developed an incentive to study and to evaluate alcohols as an alternative fuel in the spark-ignition engines. Ethanol can be fermented and distilled from biomasses, which can be considered as a renewable energy [5]. As a fuel for spark-ignition engines, alcohol has numerous advantages such as better anti-knock characteristics and reduction of CO and unburned hydrocarbon emission compared to gasoline [6]. In principle, ethanol is a promising oxygenated fuel. At the early stage, poor fuel economy and low ignitability were the main barriers to apply ethanol fuel in diesel engine [6,7]. Since the late 1990s, ethanol blended diesel fuel has been used on heavy-duty and light-duty diesel engines in order to modify their emission characteristics [8]. For example, the ethanol–diesel blends with 10% and 15% ethanol could reduce particulate matter emissions by 20–27% and 30–41%, respectively. The blends containing 83–94% diesel fuel, 5–15% ethanol, 1–3% additives and a small amount of commercially available cetane improver (0.33% by volume) in the mixture could reduce 41% particulate matter, 27% CO emission from a heavy-duty diesel engine as established in laboratory and field tests [9,10]. However, a small amount of formaldehyde, acetaldehyde and acetone was found in the emission of using methanol–gasoline blended fuels. Although the emission of aldehydes was found in exhaust, and the damage to the environment by emitting aldehydes is much less than that by poly-nuclear aromatics exhausted from burning of gasoline. Briefly, a higher percentage of alcohol in blended fuel can make a better air quality in comparison with gasoline [7,11–13]. Recent FTS has been considered as a part of gas-to-liquids (GTL) technology, which converts natural and associated gases to more valuable middle distillates and lubricants [14]. A summary of GTL projects which were realized in last decades are tabulated (Table 1). From the literature review, it is noticed that alcohol–gasoline blended fuels can effectively lower the pollutant emission without major modification to the engine design [5,15]. Finding an efficient way to produce higher alcohols from syngas is still an interesting challenge. Different routes to obtain bio-energy from biomass mapping and fuel products, position has sketched in Fig. 1, adopted from our early studies by Mohanty et al. [16].

There are five different kinds of thermochemical conversion i.e. combustion, gasification, liquefaction, hydrogenation and pyrolysis discussed in Tables 2 and 3 [11,12]. Among these methods pyrolysis is widely accepted because it can convert biomass directly into solid, liquid and gaseous products by thermal decomposition of biomass in the absence of oxygen. The first industrial FTS catalyst and the first industrial plant came into existence during world war-II and dedicated to this process at Germany by Ruhrchemie AG in 1936, plant facilities

Table 1
Recent GTL project throughout the globe [11,12].

Location	Company	Productivity (barrel/day)	Current status
Mossel Bay, South Africa	Petro SA (SASOL technology)	30,000	In operation since 1991
Bintulu, Malaysia	Shell	12,500	In operation since 1993
Oryx, Qatar	Sasol	34,500	Inaugurated in 2006, start up
Pearl, Qatar	Shell	140,000	Under construction
Escravos, Nigeria	Sasol Chevron	34,000	Under construction

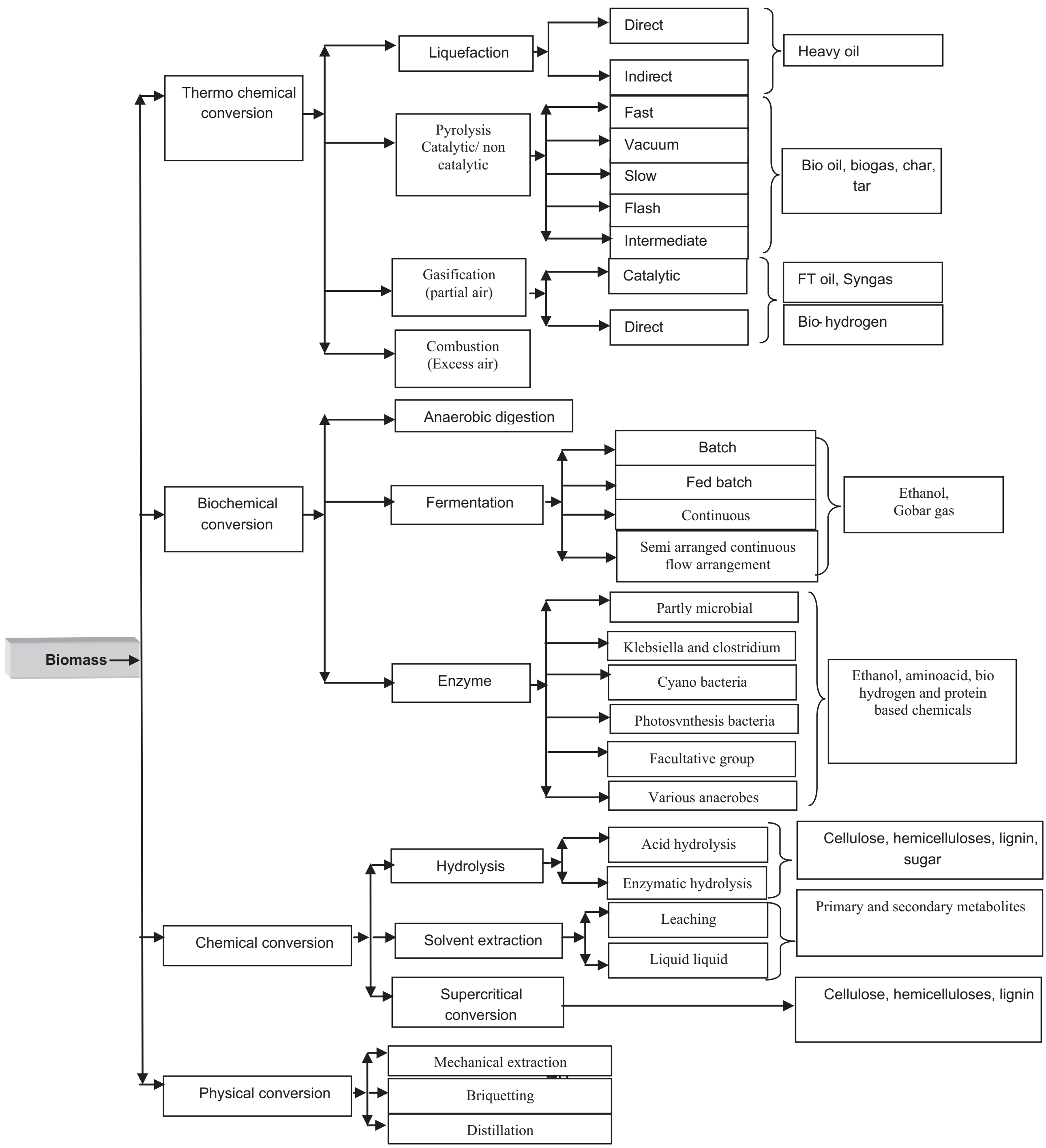


Fig. 1. Different routes to obtain bioenergy, biooil, syngas and green fuel utilizing different sources of biogenic waste/biomass adopted from Mohanty et al. [16].

utilized fully to avoid the synthetic fuel scarcity during the war, but after that it came to a closure [11,12]. Biomass gasification and subsequent catalytic FTS are key technologies for second generation automotive biofuels production. However, this promising combined process is still far from commercialization and only pilot plants are available at the time, most of them being

Table 2
Biochemical and thermochemical process comparision in terms of yield and energy content [11,12].

Process	Biofuel Yield (liters/dry wt. ton)		Energy Content (MJ/L)	Energy yield (GJ/ton)	
	Low	High	Low heat value	Low	High
Biochemical (Enzymatic hydrolysis ethanol)	110	300	21.1	2.3	6.3
Thermochemical Syngas to FT diesel	75	200	34.4	2.6	6.9
Syngas to ethanol	120	160	21.1	2.5	3.4

Table 3
Different thermo-chemical processes description [11,12,16].

Different thermo-chemical processes	Description	Remark
Combustion	The biomass is directly burnt in the presence of air to convert chemical energy stored in biomass into heat, mechanical power, or electricity, etc.	Combustion is feasible only for biomass with moisture content of 50%. It requires some pre-treatment like drying, chopping, grinding, etc., which in turn is associated with financial costs and energy. Expenditure.
Gasification	In this process, biomass is converted into a combustible gas mixture by the partial oxidation of biomass at high temperature, in the range 800–900 °C.	It gives products in gaseous form. So it requires after treatments to get the desired products which is associated with extra cost.
Liquefaction	In this process, liquid is obtained by thermo-chemical conversion at low temperature and high pressure using a catalyst in the presence of hydrogen.	It is an expensive process and also the product is a tarry lump, which is difficult to handle.
Hydrogenation	This process is mainly for the production of methane by hydro-gasification, i.e., first the syn-gas is formed and then CO is reacted with H_2 to form methane.	Same as gasification
Pyrolysis	Pyrolysis is defined as the thermal degradation of biomass in the absence of air to produce char, pyrolysis oil or syngas. pyrolysis of biomass starts at 350–550 °C and goes up to 700 °C. Different conditions like temperature, type of biomass, pressure, etc. leads to formation of products in different proportions.	This method is widely accepted as it can give solid, liquid and gaseous products at one time. It requires few seconds for conversion of biomass to bio oil.

situated in Europe, US, some partners focusing on India as stated in Table 4 [11,12].

The scarcity of these plants is due to the fact that the promising biomass-to-liquid fuel process is still under extensive investigation and optimization for its best utilization. However, the combination of the processes that constitute the thermo-chemical biomass conversion route along with the different choices for systems and operating parameters make the development of an economic and viable system a rather difficult and demanding task. For example, the choices of the type of gasifier or the operating conditions prevailing to determine the CO_2 emission profile that, in turn, is also determined by the type of raw material (i.e. its classification as a waste product or an energy crop). These choices also directly affect the overall investment and operating costs, a parameter with utmost importance when discussing about new and developing technologies. Nevertheless, in order to exploit the maximum efficiency of such process, all the potential interactions between the various processing steps and also the flexibility that the process should have been taken into consideration. The above are determined by the variability of demand, prices and feedstock availability. A target like this can only be achieved through the rigorous optimization of an integrated biomass conversion scheme. Although some international studies and reviews deal with biomass and their production towards second generation biofuels through thermo-chemical conversion processes [12], sometimes extending its scope with co-production of energy through gasification combined cycles [11,13] or employing fuel cell technology [16,17], has addressed the issue of integrated thermo-chemical conversion systems for the production of liquid bio-fuels. The main processing steps for the conversion technology are presented and process modeling studies and optimization approaches which are mandatory for the determination of the optimal operating range of each processing steps are discussed further.

2. Mechanisms of FTS

2.1. Thermodynamics of liquid hydrocarbon synthesis

The alcohol synthesis reaction, in general, is constituted of several parallel and consecutive steps. The following reactions are supposed to be: Fischer–Tropsch reactions, methanol synthesis, higher alcohol synthesis reactions and the water–gas-shift (WGS) reaction, etc. [8,16]. In order to throw more light upon the chemistry of alcohol products, it is necessary to calculate the free energy of formation of some typical aliphatic alcohols [17]. Methanol is always a major product in alcohol synthesis from syngas though ethanol is more dominant in some cases [18]. The formation of methanol from synthesis gas containing CO is an equilibrium-limited exothermic reaction according to the following equations:

$$CO_{(g)}+3H_{2(g)}\rightarrow CH_{4(g)}+H_2O_{(g)} \qquad AG^{\circ}=-34.0\ \text{kcal/mol} \quad (1)$$

$$CO_{2(g)}+4H_{2(g)}\rightarrow CH_{4(g)}+2H_2O_{(g)} \qquad AG^{\circ}=-27.15\ \text{kcal/mol} \quad (2)$$

$$CO_{(g)}+H_2O_{(g)}\rightarrow CO_{2(g)}+H_{2(g)} \qquad AG^{\circ}=-6.84\ \text{kcal/mol} \quad (3)$$

$$CO_{(g)}+2H_{2(g)}\rightarrow CH_3OH_{(g)} \qquad AG^{\circ}=-6.03\ \text{kcal/mol} \quad (4)$$

$$CO_{2(g)}+3H_{2(g)}\rightarrow CH_3OH_{(g)}+H_2O_{(g)} \qquad AG^{\circ}_{298}=0.81\ \text{kcal/mol} \quad (5)$$

Table 4
Different company/institute involvement for synthetic biofuel production in global context [11,12].

Company/Institute name	Location	Type	Start up	Output
Vienna Univ. of Technology	Gussing (Austria)	P	2005	0.02 T/day
Forschungszentrum Karlsruhe GmbH	Karlsruhe (Germany)	P	U/Const	608 T/day
CHOREN Tech.GmbH	Freiberg (Germany)	P	2003	1001 T/day
Cutec	Clausthal - Zellerfeld (Germany)	P	1990	0.02 T/day
CHOREN Tech.GmbH	Schwedt (Germany)	C	2010	$2^{*}10^{5}$ T/day
ECN	Petten (Netherlands)	P	2011	346 T/day
ECN	Alkmaar (Netherlands)	D	Planned	28,800 T/day
NSE Biofuels,NESTE Oil and Stora Enso JV	Vakaus (Finland)	D	2009	656 T/day
Research Triangle Institute	N. Carolina (USA)	P	Planned	22 T/day
GTI Gas Technology Institute	Illinois (USA)	P	2009	26 T/day
Flambeau River Biofuels LLC	Wisconsin (USA)	P	2011	5.1×10^{4} T/day
Clenergen India Private Limited	Tamilnadu (India)	C	2010	100 T/day
Jindal Steel & Power Ltd	Odisha (India)	C	U/Const	80,000 bpd
Jindal Steel & Power Ltd	Angul, Odisha (India)	C	U/Const	225,000 Nm^3/h (coal–syngas)
Reliance Industries Ltd	Gujarat, India	C	U/Const	Petcoke and coal–syngas
Tata-Sasol	Srirampur, Odisha (India)	C	U/Const	80,000 bpd
Rashtriya Chemicals and Fertilizers	Talcher (Odisha)	C	U/Const	coal to ammonia–urea
Sinopec Great Wall Energy Chemical Co., Ltd. China,	China	C	U/Const	coal-to-chemical
Shell Company	Three coal gasification plants in Ukraine	C	U/plan	
DKRW plant, Houston-based company,USA	Houston, USA	C	U/Plan	Coal to gasoline, 10,600 bpd
DKRW plant,	Southern West Virginia,USA	C	U/Plan	Coal to gasoline, 33,000 bpd
TransGas plant,	USA	C	U/Plan	Coal to gasoline, 18,000 bpd

C= Commercial plant, D=Demo plant, P=Pilot plant.

Inspection of the change in Gibbs free energy of these reactions indicates that formation of methane is very dominant thermodynamically compared to the other reactions and thus methane is always a major product over the range of conditions evaluated [19–21]. Although Gibbs free energy of methanol synthesis is close to that of water–gas-shift reaction, conversion of CO and CO_2 to methanol is dependent on pressure. Synthesis of methanol increases with an augmentation of pressure. The maximum conversion, which can be obtained for a gas stoichiometry with respect to methanol synthesis, decreases as the CO content increases [9,22]. Comparing the ΔG° values for different products produced from syngas ($CO+H_2$) indicates that hydrocarbons are more favored than alcohols [7,9].

2.2. FTS as a polymerization process

FTS is a polymerization process involving the coupling of carbon–carbon bonds to form higher hydrocarbons and oxygenates [15,23–28]. The product distribution of FTS follows a monomer addition mechanism initially postulated by Flory and others [29–35] and is referred to as the Anderson–Schulz–Flory (ASF) distribution as:-

$$W_n = n(1-\alpha)^2 \times \alpha^{(n-1)} \tag{6}$$

$$\alpha = \frac{m_{n+1}}{m_n} = \frac{r_p}{(r_p+r_t)} \tag{7}$$

where n is the number of carbon atoms, w_n and m_n are the weight and mole fractions of products containing n carbon atoms, α is the chain growth probability, r_p and r_t are the rates of chain propagation and termination. Values of n are typically observed to range from 1 to 150. Eq. (6) predicts that w_n goes through a maximum with increasing n while Eq. (7) predicts that the mole fraction m_n decreases with increasing n. Thus the FTS process is not selective to a single reaction product or to a narrow range of carbon numbers, (methane is the only exception). It is observed that the selectivity range in FTS is influenced by reaction conditions such as temperatures, pressures and feed composition. High pressures (25–40 bar), low temperatures (493–523 K) and low H_2/CO ratios favor the formation of waxes, while low pressures and higher temperatures favor the formation of methane and low molecular weight hydrocarbons [36–38]. Although the ASF model predicts hydrocarbon selectivity in FTS fairly well, deviations from ASF distributions of products from FTS are observed [38–44]. Such deviations include higher than expected C_1 selectivity, lower than expected C_2 selectivity, and chain-length-dependent chain growth probability, leading to higher than expected probabilities for heavier hydrocarbons.

Various theories and models have been proposed to explain these deviations from ASF. Many of them included a two-active-site model [45], diffusion-enhanced olefin re-adsorption [46–48], solvent-enhanced olefin re-adsorption [49] due to the greater solubility of larger olefins [50] and/or greater physisorption strength of higher olefins [51], and vapor–liquid equilibrium phenomena [52]. Buchang and Davis concluded from their analysis of accumulated products in FTS that previously reported α value might be in error, thereby explaining reported deviations from ASF [15].

2.3. Mechanistic aspects of FTS

Hundreds of elementary steps have been proposed to occur during FTS with the steps either in series or in series/parallel with each other resulting in the formation of the various reaction products. As illustrated below, these elementary reactions can be divided into three steps; namely: adsorption steps, surface reactions or Langmuir–Hinshelwood reactions and desorption steps. In some cases, Eley–Rideal type of reactions have been proposed as well.

2.3.1. Hydrogen adsorption

$$CO_{(g)} + * \rightarrow CO^* \tag{8}$$

$$H_{2(g)} + 2\hat{*} \rightarrow 2H^* \tag{9}$$

Hydrogen gas is believed to be the first to physisorb and then dissociate on transition metal (Fe, Cu, or Co) surfaces at low temperatures [6,56–71]. However, at FTS reaction temperatures, the rate of hydrogen physisorption is so fast that it is difficult to separate the physisorption step from the dissociation step. Hence hydrogen temperature programmed desorption experiments and theoretical calculations show H_2 gas adsorbing dissociatively on transition metal surfaces [59–61] as shown in Eqs. (8) and (9).

Density functional theory (DFT) calculation on Fe (110) by Curulla-Ferre et al.; and Huang et al. [31,32,58] indicated that H adsorbs on-top sites. Hydrogenation and H- transfer reaction scheme as per

$$CO^* + H^* \rightarrow CHO^* + * \quad (10)$$

$$C^* + H^* \rightarrow CH^* + * \quad (11)$$

$$H_2C = CH^* \rightarrow H_3C{-}C* \quad (12)$$

$$^*H_2C = CH_2^* \rightarrow H_3C{-}CH^* + * \quad (13)$$

2.3.2. Carbon monoxide adsorption and dissociation

CO adsorption and dissociation on Fe have been studied using density functional theory (DFT), spectroscopic, and temperature programmed adsorption and desorption techniques [31,32,72]. Studies by various researchers such as Curulla-Ferre et al. and Huang et al. on a Fe (110) surface indicate that CO adsorbs on four high-symmetry sites, namely: long-bridge, quasi-threefold, short-bridge, and on-top sites [31,32,57–58,72].

$$CO^* + * \rightarrow C^* + O^* \quad (14)$$

$$CO^* + H^* \rightarrow C^* + OH^* \quad (15)$$

Their studies also show that the site of preference is dependent on CO coverage. Similarly, at temperatures similar to those of FTS, CO adsorb on transition metal surfaces (Fe, Cu, or Co) both molecularly and dissociatively [59,61,66,67,69,71] as shown in Eqs. (14) and (15) respectively. The ease of CO dissociation is facilitated by the availability of vacant sites for the dumping of the dissociation products [68]. It is being reported that CO dissociation was facilitated with increasing heat of CO adsorption [72,73]. The presence of other adsorbates such as carbon, oxygen, and hydrogen lowers the CO heat of adsorption. Boden et al. in their study of CO adsorption and dissociation on potassium-promoted Fe (110) using ultra-high resolution spectroscopy (UPS), X-ray photoelectron spectroscopy (XPS), atomic emission spectroscopy (AES) and flash desorption techniques observed that CO adsorbs molecularly at room temperature with a heat of adsorption greater than that of un-promoted Fe (110). They also reported an increased ease of CO dissociation with increased potassium promotion on Fe (110) [74]. In fact, the subject of CO adsorption and dissociation has been studied extensively especially on well-defined single crystal surfaces. It however remains a subject of controversy on whether CO dissociation, especially on Fe catalyst, is facile or whether CO dissociation is assisted by hydrogen, as it has been suggested by some other articles [73–79].

2.3.3. Reactions of undissociated CO

Molecularly adsorbed CO has been proposed to undergo hydrogenation by adsorbed H to form formyl and alcoholic intermediates [6,80–82] as shown below:

$$CO^* + H^* \leftrightarrow CHO^* \quad (16)$$

$$CO^* + H^* \leftrightarrow COH^* \quad (17)$$

2.3.4. Reactions of adsorbed C, O, and OH with adsorbed H

Adsorbed C species can react with adsorbed H species to form a CH intermediate which is subsequently hydrogenated to CH_2 and CH_3 species according to:

$$CO^* + H^* \leftrightarrow CH^* + * \quad (18)$$

$$CH^* + H^* \leftrightarrow CH_2^* + * \quad (19)$$

$$CH_2^* + H^* \leftrightarrow CH_3^* + * \quad (20)$$

McCarty et al. has proposed that about four forms of C species exist on the surface of Ni catalyst during methanation reactions [39,83]. Some of these C species could be hydrogenated at FTS reaction temperatures while others are difficult to hydrogenate except at elevated temperatures. Bartholomew et al. has proposed that carbon hydrogenation is a slow step and could be one of the rate determining steps in FTS [27]. Adsorbed O species could react with adsorbed H species to form adsorbed hydroxyl species. Although this reaction could be one of the rate determining steps for Fe and Co catalysts, whereas Iglesia has proposed that this reaction is not kinetically favorable, especially on Co [20,84]. Hydrogenation of adsorbed OH species by adsorbed H to form H_2O is believed to be the reaction leading to the formation of water. Similarly the desorption reaction scheme can be expressed as

$$R{-}CH_3^* \rightarrow R{-}CH_3 + * \quad (21)$$

$$R{-}CH = CH_2^* \rightarrow R{-}CH = CH_2^* + * \quad (22)$$

2.3.5. C–C coupling reactions

Coupling of carbon species is proposed to be the building block for chain growth. However, the form of the monomeric carbon species (C, CH, CH_2, and CH_3) has remained a source of controversy.

$$CH_2^* + CH_2^* \rightarrow {}^*H_2C = CH_2{}^* \quad (23)$$

$$CH_3^* + CH_2^* \rightarrow H_3C{-}CH_2{}^* \quad (24)$$

$$CH^* + CH_2^* \rightarrow H_2C = CH^* \quad (25)$$

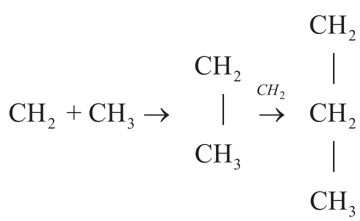
Froseth et al. depicted that C_2+ species are formed by the coupling of CH_2/CH_2 species or CH_2/CH_3 species with CH_2 species as the monomeric species [44]. Lin et al. on the other hand has suggested that coupling is between C and CH_2/CH_3 species followed by migratory insertion of H at α carbon as shown in Eqs. (23)–(25) [85]. Nevertheless, it is obvious that the formation of C_2+ species will require a form of coupling of carbon species. Mainly three mechanisms are commonly referred as the carbide or carbine mechanism, the hydroxycarbene or enol mechanism, and the
CO-insertion mechanism.

2.4. Carbide mechanism

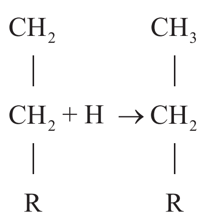
The carbide or *carbene mechanism* was proposed by Fischer and Tropsch in 1926 [86]. In this mechanism, adsorbed CO is dissociated to C and O; the carbide is then hydrogenated to CH_x (the monomer). The methylene monomer polymerizes to surface alkyl species that terminate to products. This mechanism is illustrated in Eqs. (26)–(29). It is widely supported despite the fact that it does not account for the formation of oxygenates. CO temperature-programmed desorption on both Co and Fe catalysts yield significant amounts of CO_2 [59,61]. This CO_2 is believed to be formed by the reaction of adsorbed CO with adsorbed O derived from already dissociated CO. Although activation energy calculations have shown that this reaction is very facile, CO_2 formation is rarely observed during FTS on Co catalyst even though the carbide mechanism suggests that CO dissociation into C and O is an important elementary step during FTS. Similarly, the binding energy of O is about 5.35 eV on Co [82] and 6.05 eV on Fe [87]. This higher O binding energy on Fe would mean that CO dissociation is more facilitated on Fe than on Co, and would lead to increased FTS rates on Fe than on Co. However, the FTS rate is much faster on Co than on Fe. The issues stated above suggest that

perhaps the carbide mechanism, although widely supported, may not necessarily be the primary mechanism of FTS.

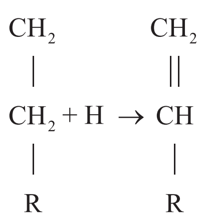
$$CO \rightarrow \underset{H_2O}{\overset{O}{\downarrow 2Hads}} + C \xrightarrow{2Hads} CH_2 \xrightarrow{2Hads} CH_3 \rightarrow CH_4 \quad (26)$$



(27)



(28)

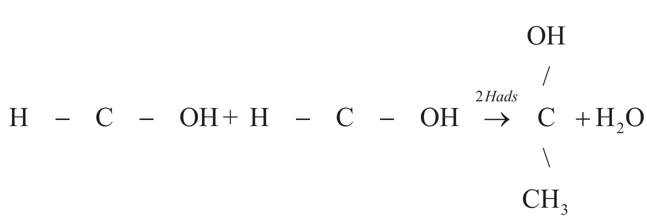


(29)

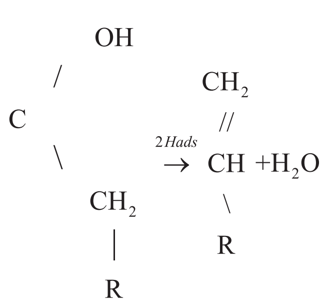
2.5. Hydroxycarbene or enol mechanism

The hydoxycarbene or enol mechanism was proposed by Epling et al. in the 1950s [86,88]. In this mechanism, chain growth is initiated through the condensation of two hydroxycarbene species CHOH-ads with the elimination of water. This is illustrated in Eqs. (30)–(33). Although this mechanism explains the formation of oxygenates and was strongly supported by Lietti et al. who has used C-alcohols or alkenes as a co-feed and observed that these alcohols participated in the chain growth [42,89], nevertheless, the details of the chemistry of this mechanism are unclear.

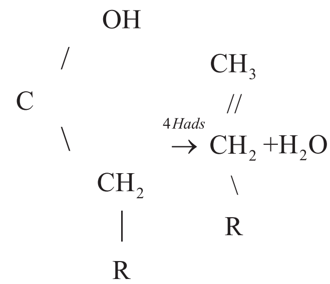
$$CO \xrightarrow{2Hads} H-C-OH \quad (30)$$



(31)



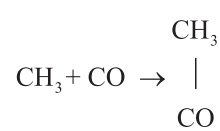
(32)



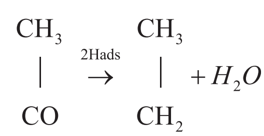
(33)

2.6. CO-insertion mechanism

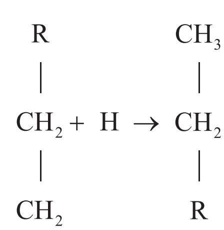
The CO insertion mechanism was proposed by Zhang et al. in the 1970s [37,90]. This mechanism involves the insertion of adsorbed CO into the methyl–alkyl bond. The oxygenated carbon is subsequently hydrogenated to remove the oxygen. CO insertion is a well known reaction in complex chemistry [91–94]; however, there is still no conclusive experimental evidence that this reaction occurs on surfaces. Jiang et al., Bian et al., and Botes [33,34,48] however suggested that, this may be the primary mechanism for iron based FTS, that is depicted as [16,18,92–94]



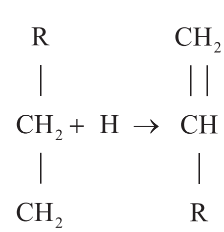
(34)



(35)



(36)



(37)

The CO conversion (%) is calculated according to the normalization method as

$$\text{CO conversion }(\%) = \frac{[(\text{Moles of } CO_{in}) - (\text{Moles of } CO_{out})]}{(\text{Moles of } CO_{in})} \times 100 \quad (38)$$

The selectivity (%) toward the individual components on carbon basis is calculated according to the same principle as

$$\text{Selectivity of } j \text{ product }(\%) = \frac{(\text{Moles of } j \text{ product})}{(\text{Moles of } CO_{in}) - (\text{Moles of } CO_{out})} \times 100 \quad (39)$$

2.7. Reactions of C and O with H

Inderwildi et al. depicted about the conversion of CO and its related kinetics [59]. The transient kinetics at 700 K and high pressure (30 bar) is a typical phenomenon. Initially $CH_2O(s)$ is formed but is rapidly depleted due to its conversion to $CH_2(s)$. Small amounts of CHO(s) are present on the surface throughout, but dissociation of this species (i.e., CH(s) formation) is not observed. This phenomenon demonstrates that the main reaction pathway is the hydrogenation of CO, yielding CHO(s) and hence $CH_2O(s)$. It is the decomposition of this species to $CH_2(s)$ that gives rise to the building block for higher hydrocarbon formation. It may be due to the dissociation reactions that are much more likely at surface defects as steps. Various studies show CO dissociation steps, as found on corrugated on cobalt (Co) is not the carbide mechanism but an alternative branch starting with the hydrogenation of CO to an oxymethylidyne species. Moreover, Gong et al. determined the dissociation barrier for CO at the steps of corrugated Co to be 1.61 eV, compared with our barrier of 1.31 eV for hydrogenation on the flat surface [58]. This information confirms our basic conclusion that CO(s) hydrogenation is the initiation step in the Fischer–Tropsch process when cobalt is the catalyst material. Adsorption followed by two hydrogenation steps successively weakens the triple bond of CO on cobalt to yield the $CH_2(s)$ building block for polymerization in the Fischer–Tropsch process. Moreover, after each hydrogenation step, the resulting species is adsorbed with its C–O bond parallel to the surface so that both oxygen and carbon are bound to the surface and activated for further hydrogenation and dissociation [15,31,32,58,93–95].

3. Summary of alcohol synthesis catalysts

Since the early 19th century, catalysts have often been referred to as the heartbeat of industrial chemical processes. Two of the largest applications of heterogeneous catalysts were petroleum refining and production of poly-olefins. Recently, catalyst development has focused on the production of liquid fuels due to the requirements of renewable energy. A number of processes have been studied to fulfill needs for catalytic conversion of synthesis gas to methanol, ethanol, and higher alcohols. The product distribution and activity of supported catalysts has been an interesting subject [60,69,70]. Furthermore, a number of higher alcohol synthesis catalysts (IFP, Dow Chemical, Lurgi, and Octamix) have been applied at commercial scale though some are no longer used [9]. The composition of such catalysts is usually based on either a monometallic component like Rh-, Ru-based catalysts or multi-component (Cu, Pt, Co, Fe, Ni, Mo, Mn, Zn, Cr, and Al). For the sake of simplification, the higher alcohol synthesis catalysts are classified into two major types: the modified methanol synthesis catalysts [62–64] and the modified Fischer–Tropsch (FT) and the group VIII metal-based catalysts [66–68,70]. Molybdenum sulfide catalyst promoted by alkali also produces a mixture of linear alcohols following an ASF distribution while Rh-based catalyst is similar but produces more C_2^+ oxygenates. Also majority of the catalysts for CO_2 hydrogenation contained Cu and Zn as the main components together with different modifiers (Zr, Ga, Si, Al, B, Cr, Ce, V, Ti, etc.) [74,75]. The following sections will focus on several representative higher-alcohol-synthesis catalyst systems that may have potential industrial applicability.

3.1. Modified methanol synthesis catalysts

The synthesis of methanol from syngas is a most active and selective industrial process that has been carried out on a commodity scale for the last three decades. The synthesis gas is mainly obtained by steam reforming of natural gas (mainly methane) at a high temperature or by gasification of coal [76]. In all cases, the resultant syngas also contains CO_2, whose low concentration may be necessary for higher conversion of syngas to alcohols [70,77]. A number of higher alcohol synthesis catalysts have been developed from the methanol-synthesis catalysts with a "zinc chromites-type" Zn/Cr spinel. Another type operating substantially at lower temperatures (523–573 K) contains a Cu–Zn–Cr component. The reaction occurs through a combination of hydrogenation and carbon–carbon bond formation via aldol condensation, giving rise to the formation of branched alcohols with a non-ASF product distribution. Those representative reactions over the catalysts can be described by

Alcohol formation:

$$nCO + 2nH_2 \rightarrow C_nH_{2n+1}OH + (n-1)H_2O \tag{40}$$

Hydrocarbon formation:

$$nCO + (2n+1)H_2 \rightarrow C_nH_{2n+2} + nH_2O \tag{41}$$

Water–gas-shift reaction equilibrium:

$$CO + H_2O \rightarrow CO_2 + H_2 \tag{42}$$

The sketch reaction in Eq. (40) shows the production of a homologous series of alcohols. There are only methanol and isobutanol formed as the major products [60,78,79]. The alcohol distribution obtained on these catalysts, however, is undesirable thus for the direct product application of methyl-tertiary butyl ether (MTBE). It happens because the methanol-to-isobutene mole ratio is somewhat high. Furthermore, a large amount of byproducts is inevitably formed. In some cases the reaction conditions result in the fast deactivation of the catalyst possibly due to sintering of the surface metals [60,80].

3.2. Modified high temperature methanol synthesis catalysts

The addition of alkali or alkaline-earth to methanol synthesis catalysts could promote the formation of higher alcohols and other oxygenates. Commercial mixed alcohol synthesis had been performed with alkalized ZnO/CnO_3 catalysts under severe conditions (high temperature and pressure) since 1930. Typical operating conditions for this catalyst are temperatures of 653–723 K and pressures of 120–250 atm and the major products are methanol and branching alcohols [80,81]. The selectivity to higher alcohols is dependent on the feed composition, temperature, pressure, etc. Both the production and the selectivity of higher alcohols obtained decrease significantly in the presence of excess hydrogen and high CO_2 feed content ($<6\%$). The formation of alcohols over these catalysts is constrained by kinetics rather than thermodynamics. Tronconi et al. reported that the formation of oxygenates occurs through a kinetically controlled chain-growth process and is favored by long contact time [82,83].

The high temperature catalysts have been very widespread during the last 20 years because of their good selectivity towards methanol and iso-butanol that are important reactants for synthesis of methyl-tertiary butyl ether. A ratio of 50/50 mol% mixture of methanol and iso-butanol is an ideal feedstock for the direct production of MTBE although this ether has been no longer blended into gasoline [84,86,88]. Recently, Epling et al. have published a series of publications bringing to light on the role of Cr, Zn components, alkali of commercial Zn/Cr spinel catalyst [86,88,96]. These authors used the ion scattering spectroscopy (ISS) and XPS techniques for a study of the surface and pointed out that the outermost surface layer of fresh catalyst consists of C, O, Cr, and Zn. After the reduction, the H_2 treatment may remove some surface oxygen exposing underlying K and/or possibly some K may migrate from the subsurface region to the near-surface region during the pretreatment. In this case, therefore, an alkali

promoter is exposed at the outermost layer. Both XPS and ISS data indicate that the K and Cr are present as K_2CrO_4 or $K_2Cr_2O_7$; on the other hand Zn is enriched on the near-surface region and present mostly as ZnO. XPS data show that both the reductive pretreatment and reaction process do not alter the chemical state of zinc [84,86,89].

The near-surface region of such catalysts consists primarily of ZnO and alkali promoters are bound to the Cr. In the absence of promoter or promoted ZnO powder (without spinel structure), the catalysts do not produce higher alcohol synthesis (HAS); however, iso-butanol is obtained as soon as K is introduced into the ZnO powder [84–88]. This result demonstrates that alkali-promoted ZnO surface may be the active catalytic phase for synthesis of higher alcohols. Furthermore, zinc oxide alone is not a good catalyst at high pressure and temperature because it is not stable and quickly loses its activity. The course of its working life can be improved by incorporation of Cr, which acts as a stabilizer preventing the growth of the ZnO crystals. Indeed, the Zn/Cr spinel catalyst with the Cr:Zn ratio of 1:1 is rather active for HAS. Addition of excess amount of ZnO to sample during preparation, however, gives rise to a significant improvement in iso-butanol production rate [86,88,92]. The Zn/Cr spinel structure only acts as a high surface area support and provides the ZnO over layer. Hoflund et al. reported that the acidity of surface Cr catalyzes the production of hydrocarbons [84]. A large amount of Cr on the surface leads to increased acidity of the catalyst and therefore enhances the formation of hydrocarbons. Consequently, the presence of Cr is probably not necessary and may even be detrimental for HAS in some cases. Thus, the addition of alkali into the catalyst inhibits the formation of hydrocarbons simply by covering the undesired acid surface Cr species. Surface studies have pointed out that the alkali is bound to the Cr elements in the near-surface region, resulting in a decrease in the formation of hydrocarbons [84,92]. Therefore, the main role of Cr is only to provide a high surface area by the formation of spinel although chromite causes the formation of some undesirable products. In order to eliminate the negative effects of chromite component on the higher alcohol synthesis catalyst, Cr was partially substituted by Mn in the spinel structure [60,88]. Thereby, it is expected that the catalyst has lower acidity and restricts to the production of hydrocarbons. Further Epling et al. partially replaced the Cr by Mn in Cs-promoted Zn/Cr spinel catalyst and observed a small decrease of hydrocarbon byproduct formation; simultaneously the methanol-to-iso-butanol mole ratio is close to the desired ratio of 1 [88]. This may imply that the substitution of Mn for Cr suppresses hydrocarbon formation in spite of no further evidences demonstrating that the presence of Mn is better than that of Cr, shown in Table 5. As mentioned above, the reactions are usually carried out under severe reaction conditions (high temperatures and pressures) and mainly yield methanol, iso-butanol, CO_2, and methane [60,81]. These conditions would require an expensive compression step for synthesis gas produced by conventional methods. Moreover, the high-temperature operation which consumes a lot of energy still tends to form appreciable yields of hydrocarbons. Therefore, the modified low-temperature methanol synthesis catalyst would be paid more attention.

3.3. Modified low-temperature methanol synthesis catalysts

Introducing Cu into ZnO/M_2O_3 methanol synthesis catalysts makes them operate under milder conditions (like lower temperatures and lower pressures). Alkali-promoted Cu/ZnO supported catalysts provide for the production of higher alcohols under moderate temperatures and pressures. The copper crystallites in catalysts have been identified as active catalytic sites although the oxidation state (oxide of metal, etc.) of the copper sites is still being debated very often [63]. It was also observed that under typical reaction conditions, the copper oxide phase was completely reduced to metallic copper [94,97]. The CuO reduction occurred in the temperature range of 490–500 K. The crystallite size of copper particles tends to increase with augmenting reduction temperature. Therefore, the ZnO and M_2O_3 (M=Cr, Al) in the catalyst formulation are suitably refractory at reaction temperatures and create a high Cu metal surface area. ZnO also interacts with Al_2O_3 or Cr_2O_3 to form the spinel which provides a robust catalyst support. Hence, chromium and alumina play the important role of structural promoters as follows: (i) decreasing the onset temperature for the reduction of segregated copper oxide; (ii) stabilizing partially oxidized copper in the reduced catalyst by the formation of $CuCr_2O_4$; (iii) stabilizing catalyst activity, in particular at higher temperatures; (iv) increasing surface acidity which results in an increase in hydrocarbon and ether selectivities [95]. Aside from providing a large surface area, the chromium support also prevents the ZnO and Cu particles from growing. However, the activity of ternary $Cu/ZnO/Cr_2O_3$ catalyst expressed per m^2 of surface area was reported to be approximately 30% lower than that of binary Cu/ZnO catalysts under the similar test conditions [95,98]. This is primarily due to the fact that the chromium provides a significant portion of the total catalyst surface area. However, these acidic materials are known to be dehydration catalysts producing ethers. By interacting with the Cr_2O_3 support material, ZnO effectively improves alcohol selectivity by reducing the potential for ether formation. Indeed, the XRD data indicated the presence of the oxides of copper, zinc, chromium and $ZnCr_2O_4$ spinel phases after calcinations. After pretreatment in hydrogen, the catalyst displayed almost the same phases with the exception of copper oxide that is reduced to metal. However, the reduction of copper is inhibited by incorporation of alkali promoter. Indeed, it was found that the presence of cesium retards CuO reduction by about 323 K on the ternary Cu–Zn–Cr oxide catalyst. This might be associated with a closer interaction

Table 5
Selected high-temperature and low-temperature methanol synthesis catalysts employed in the direct conversion of Syngas to ethanol and mixed alcohols.

Catalyst	Experimental conditions					
	Temp (°C)	Press (psig)	GHSV (h^{-1})	H_2/CO	X_{CO} (%)	Ref.
K_2O–Pd–ZrO_2–ZnO–MnO	400	3626	99,000	1.0	NA	[79]
4 mol% Cs–ZnO–Cr_2O_3	405	1100	18,000	0.75	4.5	[122]
3 wt% Cs–5.9 wt% Pd–ZnO–Cr_2O_3	440	1500	NA	1.0	19.0	[123]
3 wt% K–5.9 wt% Pd–ZnO–Cr_2O_3	440	1500	NA	1.0	14	[91]
3 mol% Cs–Cu–ZnO–Cr_2O_3	325	1100	5450	0.75	19.7	[88]
3 mol% Cs–Cu–ZnO–Cr_2O_3	325	1100	12,000	0.75	13.8	[122]
3 mol% Cs–Cu–ZnO–Cr_2O_3	325	1100	18,000	0.75	11.7	[91]
3 mol% Cs–Cu–ZnO–Cr_2O_3	310	1100	5450	0.45	20.2	[122]

between the CuO phase and promoter which inhibited H_2 dissociation and the nucleation of Cu°. The promotion of Cu/ZnO and $Cu/ZnO/M_2O_3$ catalysts with alkali causes the rate of conversion and the selectivity towards alcohols to go through a maximum as a function of promoter concentration. Smith et al. has also observed an increase in the higher alcohol selectivity with the addition of potassium to the $Cu/ZnO/Al_2O_3$ at 533–573 K and 100 atm [94,96]. This is explained by the bi-functional character of these catalysts (hydrogenation and basicity). Alkali addition is to promote the selectivity of alcohols (1-propanol, 2-methyl-L-propanol, and 2-methyl-L-butanol) and to reduce the formation of hydrocarbons and dimethyl ether. XPS results indicated the alkali ion being uniformly spread onto the surface as a sub-monolayer. Wherein, promoters have a double effect: (i) elimination of surface acidity leading to suppression of DME formation, (ii) improvement in the carbon–carbon bond formation between surface species on basic sites. Additionally, doping with cesium results in an increase in the stability and the suppression of the synthesis of dimethyl ether, but at high cesium loadings the alcohol synthesis is inhibited because alkali species cover the majority of the hydrogenation centers on the catalyst surface. Smith et al. has indicated that the HAS selectivity was improved significantly by promoting the catalysts with alkali and by carrying out the synthesis at higher temperatures and lower H_2/CO ratios [96]. The oxygenated products were promoted including methanol, ethanol, 1-propanol, 2 methyl-1-propanol, 1-butanol, and 2-methyl-L-butanol and a small amount of aldehydes, secondary alcohols, ketones, ethers. Hydrocarbons, CO_2, and H_2O are unavoidable byproducts due to the occurrence of water–gas-shift reaction. In order to decrease the formation of undesired products, the synthesis reaction is favored by operating at a low H_2/CO ratio (<2), a small CO_2 feed content ($<1\%$), a low gas hourly space velocity(GHSV) value (2.00–4.00 h^{-1}), and appropriate reaction temperatures (503–583 K) [60,97–99].

3.4. Dual catalyst bed reactors for higher alcohol catalysts

Consideration of two modified methanol synthesis catalysts presented above shows that the major products of CO hydrogenation are methanol and branched alcohols, methane and CO_2. Once formed, isobutanol is stable and does not react further in the carbon chain growth because of its steric hindrance and the lack of two a-hydrogens required for aldol condensation reactions [62,64,96,98]. Klier et al. and Nunan et al. have indicated that the rate-determining step is the $C_1 \rightarrow C_2$ step which initiates the chain growth process, and by virtue of its low rate limits the production of higher alcohols [77,98]. This is strongly supported by the results of the addition of lower alcohols to the stream feed leading to an enhanced productivity of higher alcohols, particularly the yield of iso-butanol [62,98]. Therefore, a high productivity of higher alcohols could be achieved if a double catalyst bed reactor was employed. In combination of the advantages between two types of modified methanol synthesis catalysts, the coupling of two catalyst beds in series at different reaction temperatures to optimize the chemistry of the different C–C bond-forming steps ($C_1 \rightarrow C_2$ step) and the subsequent growth steps was proposed by Klier's group [77,78,95]. The concept of the double bed configuration is based on the two catalyst layers, where in the top bed ($Cu/ZnO/Cr_2O_3$) supplied methanol and C_2–C_3 intermediate oxygenates that were then converted to branched alcohols over the second layer [100–104]. Therefore, a double bed catalyst system was designed to contain two layers. The first bed was the $Cs–Cu/ZnO/Cr_2O_3$ and the second one was the copper-free $Cs–ZnO/Cr_2O_3$ taken in dual step reaction scheme. The top catalyst layer (step 1) operated at low temperature produces mainly methanol while the second one (step 2) is designed for both maintaining a high feed rate of methanol and rapid conversion into higher molecular weight products [105–109]. Using a double-bed reactor configuration ($H_2/CO=0.75$; 7.6 MPa; GHSV$=$18,375 l/kg_{cat}/h), Majocchi et al. obtained a higher productivity of isobutanol as compared with only utilizing either $Cs/Cu/ZnO/Cr_2O_3$ (at 598 K) or free-copper zinc chromite catalyst (at 678 K) shown in Table 6 [97–100]. However, both methanol and isobutanol are direct reactants for production of MTBE, which has been phased out as a gasoline additive. So, the modified Fischer–Tropsch catalysts have recently become more attractive instead of the modified methanol catalysts because of their ability to produce a mixture of linear primary alcohols [101–108].

3.5. Modified Fischer–Tropsch catalysts

As a general rule, the processes based on the Fischer–Tropsch catalyst are not that much selective due to the formation of a mixture of olefinic, paraffinic and oxygenated products [99,110–113]. A large number of catalysts have been reported to be quite active for the selective conversion of syngas into higher alcohols, but in actual fact the results do not corroborate the claims in various reports. Generally, higher alcohol synthesis catalysts are consisting of some elements selected from groups IB, VIB, VIIB, and VIIIB, shown in Table 7 [65,114–127]. Apart from a catalyst based on thorium, most of the higher alcohol synthesis catalysts comprised an alkali metal as a promoter.

3.6. Rhodium based catalysts

During early research efforts by Fischer and Tropsch, it was discovered that ail group VIIIB metals catalyze CO hydrogenation. The activity and selectivity are different for each metal, depending

Table 6
Fischer–Tropsch bifunctional catalysts [100–109].

Catalyst	Rh/Zr/Mg	Rh/Mg/Cs	Cu/Co/Cr/La/K	Fe–Mn–Ru	H–Ga–silicate	Rh/Ti/Fe
Temperature, K	548	548	523	593	823	533
Pressure, bar	100	20	60	20	Atmosp.	50
$CO:H_2$	1:1	1:1	1:3.5	1:1	1:1	1:1
CO conv. (%)	36	38	32	30.3	27.3	33.5
Products (wt%)						
Ethanol	87.6	9.4	35.8	10.3	23.0	71.6
Acetaldehyde	4.4	35.8	–	–	–	4.6
Acetic acid	7.8	54.8	–	–	–	19.8
Methanol	–	–	17.6	28.2	32.4	4.0
1-propanol	–	–	27.0	17.3	21.6	–
1-Butanol	–	–	19.6	33.5	0.3	–
Aromatics	–	–	–	–	19.1	–

Table 7
Selected Cu Co-based catalysts patented by IFP for the direct conversion of syngas to ethanol and mixed alcohols.

Catalyst	Experimental conditions					
	Temp (°C)	Press (psig)	GHSV (h^{-1})	$H_2/(CO+CO_2)$	X_{CO} (%)	Ref.
$Cu_{1.0}Co_{1.0}Cr_{0.8}K_{0.09}$+cement	250	870	4000	2.0	NA	[91]
$Cu_{1.0}Co_{1.0}Cr_{0.8}K_{0.09}$+cement	250	1740	4000	2.0	NA	[125]
$Cu_{1.0}Co_{1.0}Cr_{0.8}K_{0.09}$+cement	250	1740	8000	2.0	NA	[91]
$Cu_{1.0}Co_{0.7}Zn_{0.3}Cr_{0.8}K_{0.09}$	250	870	4000	2.0	NA	[126]
$Cu_{1.0}Co_{1.0}Cr_{0.5}La_{0.3}K_{0.09}$	250	870	4000	2.0	NA	[125]
$Cu_{1.0}Co_{1.0}Mn_{0.8}K_{0.12}$	250	870	4000	2.0	NA	[92]
$Cu_{1.0}Co_{1.0}Fe_{0.8}K_{0.12}$	250	870	4000	2.0	NA	[126]
$Cu_{1.6}Co_{1.8}Cr_{1.6}+H^{+}$–ZSM-5	275	1000	600	1.0	46	[92]
$Cu_{3.2}Co_{3.6}Cr_{3.2}$	375	1350	600	1.0	66	[91]
Fe–Cu–K/ZSM-5 (SAR=25)	300	147	2000	2.0	80.7	[127]
Fe–Cu–K/ZSM-5 (SAR=40)	300	147	2000	2.0	78.9	
Fe–Cu–K/ZSM-5 (SAR=140)	300	147	2000	2.0	61.1	

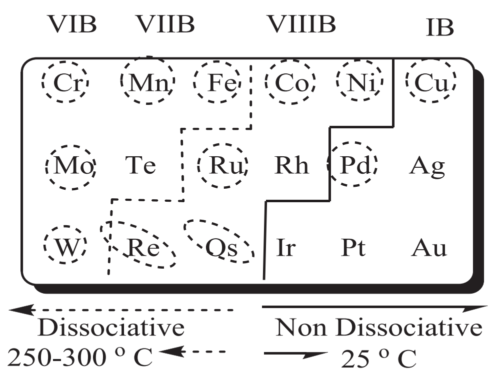


Fig. 2. Predominant form of CO adsorption over transition elements.

Table 8
Selected Rh-based supported catalysts employed in the direct conversion of syngas to ethanol.

Catalyst	Experimental conditions					
	Temperature (°C)	Pressure (psig)	GHSV (h^{-1})	H_2/CO	X_{CO} (%)	Ref.
$RhCoFeK/SiO_2$	281	900	3000	1.0	6.8	[128]
$RhCe/SiO_2$	350	1 atm	300	1.7	NA	[129]
$RhMo/ZrO_2$	210	300	2400	1.0	10	[91]
$1\%Rh/V_2O_5$	220	1 atm	NA	1.0	4.5	[130]
$1\%Rh/ZrO_2$	220	1 atm	NA	1.0	2.0	[131]
$1\%Rh–SmV/SiO_2$	280	435	13,000	2.0	5.4	[91]
$6\%Rh1.5\%Mn/SiO_2$	300	783	3750	2.0	40.5	

on its ability of adsorption and dissociation of CO. The main reason for this is the predominant way in which they adsorb CO. As seen from Fig. 2, metals to the left of an imaginary line drawn from between Fe and Co to those between W and Re in the periodic table, readily dissociate CO at room temperature. At higher temperatures, where CO hydrogenation usually occurs, the line shifts to the right. Elements to the right of the solid line are not good catalysts for the formation of hydrocarbons and higher alcohols, although some could produce methanol [68,69]. Meanwhile, elements to the left of group VIIB do not catalyze CO hydrogenation mainly because they could form so stable carbides or oxides that they become inactive for the CO conversion into hydrocarbons and oxygenates. Thus, in order to prepare a higher alcohol synthesis catalyst which could catalyze the formation of C–C bonds (propagation), the hydrogenation and insertion of CO to terminate the polymerization, the catalyst could be designed by either combining two (or more) elements like Co–Cu catalysts or by single metal which is capable of adsorbing CO both dissociative and non-dissociative [68]. In the group VIIIB metals, nickel is a catalyst producing almost exclusively methane due to its ability to dissociate CO (ΔE. CO_g=25 KJ/mol^{-1}) [36,128]. On iron and cobalt which are known as typical excellent Fischer–Tropsch catalysts, stronger metal–carbon bonds lead to C_{2+}-hydrocarbon formation, yielding a mixture of linear parrafins and a-olefins [14,96]. In addition, the predominant phase of Fe-based catalysts under actual reaction conditions is the carbide although the oxide Fe_3O_4 is also present, but no Fe metal is observed at high H_2O/H_2 ratios. Ruthenium is a very active but expensive catalyst for the Fischer–Tropsch synthesis relative to Co and Fe. At relatively low pressure ($P<100$ bar), ruthenium produces much methane, whereas at low temperatures and high pressure it is selective to high-molecular-weight waxes [68]. The molecular mass of polyethylene could reach 1 million at low temperature (373 K) and high pressure (1000–2000 bar) [23,128]. In brief, Vannice has determined the activity of group VIII metals supported on AbOs-silica in CO hydrogenation and reported a decrease in activity in the order Ru, Fe, Co, Rh, Pd, Pt, and Ir [101]. This is in agreement with the fact that Rh lies in an intermediate position, which is capable of adsorbing CO both dissociative and non-dissociative. Therefore, Rh is expected to be a versatile CO hydrogenation catalyst for the synthesis of both hydrocarbons and oxygenates, as discussed in Table 8 [65,102]. Indeed, Rh presents a great versatility in the syngas reactions and is able to catalyze the formation of alcohols and hydrocarbons possibly with governed selectivity.

According to literature, the activity and the selectivity reported over Rh-based catalysts are strongly dependent on the types of supports, promoters, rhodium precursors, and reaction conditions [102,105]. For instance, Rh supported on silica produces only methane and a small yield of higher hydrocarbons, but Rh/SiO_2 containing some impurities (Na, Fe) become active for the synthesis of oxygenates. Using basic supports such as ZnO, MgO and CaO shifts the selectivity toward methanol. Meanwhile, transition metal oxide supports including ZrO_2, MnO, TiO_2, Nb_2O_5, rare earth oxides, CeO_2, Nd_2O_3, and La_2O_3 for example, produce mainly ethanol and small methanol, acetaldehyde, acetic acid, and ethyl acetate [105]. The fluctuation in the selectivity of Rh-based catalysts is possibly due to a strong electronic interaction between the Rh and oxide supports that affects the electronic state of Rh. From literature it has been found that the binding energy of Rh over MgO obtained by reduction under 350 torr of H_2 at 473 K for 1 h positioning at 308.4 eV which is very close to the mean value of the Rh^{+} ions. In this case, 94% of the CO was converted into methanol product. On the contrary, $RhZrO_2/SiO_2$ showing the

binding energy of Rh $3d_{5/2}$ of 307.7 eV which characterizes to the presence of both Rh° and Rh^{+1} states produces almost ethanol together with a small amount of methanol and hydrocarbons. This is consistent with the $LaRhO_3$ results for CO hydrogenation reported by [103]. Also it has observed that the coexistence of Rh^{+n} and Rh° acting as active centers for oxygenate synthesis [102,103]. In addition, alkali metal compounds introduced as oxides, carbonates, hydroxides enhance in the selectivity toward ethanol although a full understanding of how promotion occurs has not been elucidated yet. Some explanations have been proposed: (I) promoters enhance the overall activity of the catalysts by improving the ability of Rh to dissociate CO; (ii) promoters partially block some CO dissociation centers that lead to an increase in the oxygenate selectivities, in other words, CO dissociation is hindered due to fewer ensembles of contiguous Rh atoms on the catalytic surface; (iii) another crucial function of the promoters is the stabilization of positive rhodium ions which are involved in the mechanistic formation of higher oxygenates, perhaps as active sites for CO intercalation [102,103]. Thus, the active surface for oxygenate synthesis was assumed to be composed of mixed metallic and oxidized Rh [91]. Subramani et al. proposed that Rh° sites function as CO dissociation sites in the formation of alkyl group while Rh^{+} ions serve as the sites for associative CO adsorption and subsequent CO insertion to form acyl species [91]. Based on the results of IR and isotope labeled experiments, many authors recently suggested that the surface acyl species is an intermediate for the synthesis of C_2-oxygenates [93]. The acyl group is very reactive and less stable under the reaction conditions compared to the acetate which is more stable. Two possible routes for the C_2-oxygenate formation have been proposed. The first is the hydrogenation of the acyl intermediate and the other is the hydrogenation of the surface acetate species. Addition of a hydrogen atom to the acyl group gives acetaldehyde, and further hydrogenation leads to the formation of the ethoxy group, and further yields ethanol. Hydrogenation of acetate leads probably to the formation of both acetic acid and surface acetaldehyde which is further hydrogenated to form ethanol. The Rh-based catalysts were usually operated at mild conditions ($T=523$ K, 2 MPa, GHSV$=6000\ h^{-1}$). In contrast to the modified methanol synthesis catalysts, the selectivity to MeOH obtained on Rh-based catalysts is very low while methane selectivity is still very high ($>40\%$); simultaneously the formation of CO_2 is rather low. Total selectivity of oxygenates including ethanol, aldehydes, acetates is about 50% [60,69]. The Rh-based catalyst is therefore considered as a selective catalyst for ethanol synthesis from syngas, but its activity is very fickle and depends strongly on the preparation route, precursors, and reaction conditions. This fluctuation of Rh-based catalyst in its properties for syngas conversion may be a major disadvantage in this respect, since small amount of poisoning, modification or sintering ails leads to a drastic effect on the product distribution. Therefore finding other catalysts of high activity and selectivity to ethanol and higher alcohols is necessary [129–134].

3.7. *Alkali-doped molybdenum sulfides*

Molybdenum disulfides are widely distributed throughout the world for use in many important applications such as the hydrodesulphurization (HDS) of petroleum. Molybdenum-containing catalysts play also an important role in hydro-treating feedstock to produce cleaner fuels, and currently as base catalysts promoted by alkali and cobalt for higher alcohol synthesis. In 1984, the Dow Chemical Company and Union Carbide Corporation independently disclosed some new catalyst systems based on molybdenum sulfides for converting syngas to linear alcohols. These catalysts were either supported transition metal sulfide catalysts or unsupported alkali-promoted Mo or MoS_2 [78,104]. Sulfide catalysts such as MoS_2 are well-known hydrogenation catalysts; however, adding alkali ions as it shifts the products to alcohols rather than hydrocarbons [60,104,118]. Several investigations have been performed for an understanding of the nature and function of the promoter atoms on the surface of MoS_2 supported catalysts has given in Tables 9 and 10. The crystalline MoS_2 is considered as a key component in the MoS_2 based catalysts. The crystal structure of MoS_2 with natural molybdenite and disclosed that the compound is hexagonal and characterized by MoS_2 layers. The molybdenum atoms occupy trigonal prismatic coordination of six sulfur atoms, with two molecules per unit cell. Within the MoS_2 layers, each S^{-2} anion is located at the center of the space formed by three Mo^{4+} cations while each Mo^{4+} cation is bound to six S^{-2} atoms at the corners of a trigonal prism. Because of the strong bonding along two dimensions and the weak bonding between MoS_2, there exist two major types of faces: base and edge planes. In essence, the MoS_2 base plane is more stable than the edge plane because the S^{-2} anions are located on the base plane and are coordinately saturated.

Moreover, the crystal structure of MoS_2 has many defect sites in the lattice. Such sites play as active centers at the edge planes instead of base planes. Tanaka et al. has investigated the activity of the edge planes of MoS_2 in hydrogenation reactions by comparing the activity between the edge and base planes [106]. After cutting single crystals into smaller pieces and examined the rates of hydrogenation on these plane crystals. The results indicated that the hydrogenation reaction takes place predominantly on the edge planes. Therefore, carbon chain of higher alcohol reaction formed on the edge planes is not excluded. However, higher alcohols are not produced on MoS_2 in the absence of an alkali promoter. This indicated that hydrocarbon is probably produced over a MoS_2, but no higher alcohols formed unless addition of alkali promote into catalyst. A small amount of alkali is required to produce an optimum yield of C_2–C_4 alcohols and to minimize the formation of hydrocarbons. The maximum in alcohol yield has been explained by the bi-functional character of the catalyst: a balance of base and hydrogenation function. The role of alkali is generally classified as either structural or chemical (or electronic), depending on its primary function. Structural promoter is to create a high surface area of catalyst while chemical promoters improve the catalytic performance [60,104]. In this case, alkali ions are assumed as chemical promoters for alcohol synthesis. The MoS_2 catalysts were found to yield about 50–70% selectivity to higher alcohols from syngas with $H_2/CO=1$ with $\sim$10% CO conversion efficiency. The activity of the catalyst is mainly associated with the presence of Mo. Both higher alcohols and hydrocarbons formed over sulfide catalysts follow an Anderson–Shultz–Flory (ASF) molecular weight distribution with similar values and significantly improve with the presence of VIIIB metals. Introduction of Co, Ni, Mn, and La into alkalized MoS_2 catalysts increases the production of ethanol and other higher alcohols because the presence of such metals promotes the homologation of methanol to ethanol [73,106,108,109]. Activity of the sulfide catalysts also depends on the catalyst support material. Admittedly, the modified Mo-based catalysts have great potential economic for commercialization due to their high resistance to sulfur compounds, and low coking rate [60]. These catalysts have the unique property of being extremely resistant to sulfur poisoning. In fact, the process requires 50–100 ppm sulfur in the feed gas to maintain the catalyst sulfide, modified to achieve a more active status; H_2S in the feed gas is also thought to moderate the hydrogenation properties of the catalyst and improves selectivity of higher alcohols by reducing methanol production as given in Table 11 [78]. Sulfide catalysts are less sensitive to CO_2 in syngas but the presence of large amounts ($>30\%$) of CO_2 diminishes the catalyst activity. A moderate

Table 9
Selected unsulfured Mo-based catalysts reported for the direct conversion of syngas to ethanol and mixed alcohols.

Catalyst	Experimental conditions					
	Temperature (°C)	Pressure (psig)	GHSV (h^{-1})	H_2/CO	X_{CO} (%)	Ref.
1%K–Co_1Mo_4ultrafine	300	870	10,000	2.0	27.5	[71]
1%K–Co_1Mo_4ultrafine	300	870	10,000	2.0	37.5	[71]
1%K–Co_1Mo_{10}ultrafine	300	870	10,000	2.0	23.7	[71]
K-β-M o_2C	300	1160	2000	1.0	23.4	[75]
K-Co-β-M o_2C	300	1160	2000	1.0	73.0	[75]
K-Co-β-M o_2C-10	300	1160	2000	1.0	36.7	[91]
K-Co-β-M o_2C-4	300	1160	2000	1.0	62.9	[91]

Table 10
Selected MoS_2 based catalysts reported for the direct conversion of syngas to ethanol and mixed alcohols.

Catalyst	Experimental conditions					
	Tempearature (°C)	Pressure (psig)	GHSV (h^{-1})	H_2/CO	X_{CO} (%)	Ref.
MoS_2	295	1050	1300	1.0	29.2	[91]
$KRhMoS_2/Al_2O_3$	327	1450	4800	2.0	11.1	[73]
$KRhMoS_2/Al_2O_3$	327	1450	14,400	2.0	5.5	[73]
$KCoMoS_2$/C-1	330	725	4800	2.0	14.5	[91]
$KCoMoS_2$/C-4	330	725	4800	2.0	11.7	[91]
$KCoMoS_2$/C-16	330	725	4800	2.0	8.7	[91]
$K_2CO_3CoMoS_2$	270	2100	2546	1.1	10.4	[107]
$LaKNiMoS_2$	320	1160	2500	1.0	33.5	[91]
$K_2CO_3NiMoS_2$	320	1160	2500	1.0	55.6	[91]
$K_2CO_3NiMoS_2$	280	1160	2500	1.0	20.6	[91]
$Cs_2CO_3CoMoS_2$/clay	320	2000	4000	1.1	28.7	[107]
$Cs_2CO_3CoMoS_2$/clay	320	2000	4000	1.1	31.9	[107]

Table 11
Selected H_2S–MoS_2 mixed feed based catalysts reported for the direct conversion of syngas to ethanol and mixed alcohols.

Catalyst	Experimental conditions					
	Temperature (°C)	Pressure (psig)	GHSV (h^{-1})	H_2/CO	X_{CO} (%)	Ref.
6%Rh 1.5% Mn/SiO_2	300	783	3750	2.0	40.5	[124]
K_2O–Pd–ZrO_2–ZnO–MnO	400	3626	99,000	1.0	NA	[91]
3 mol% Cs-Cu–ZnO-Cr_2O_3	325	1100	18,000	0.75	11.7	[122]
Cu1.0Co1.0Cr0.8K0.09+cement	250	1740	8000	2.0	NA	[91]
K–Co-β–Mo_2C-10	300	1160	2000	1.0	36.7	[75]
$K_2CO_3CoMoS_2$	270	2100	2546	1.1	10.4	[91]
$Cs_2CO_3CoMoS_2$/clay	320	2000	4000	1.1	28.7	[107]
K/MoS_2	320	120	2500	1	22.49	[133]
Ni/ADM (ADM, K/Mo molar ratio=0.7)	320	120	2500	1	39.65	
La/Ni/ADM (ADM, K/Mo molar ratio=0.7)	320	120	2500	1	33.52	

concentration of CO_2 ($<7\%$) in syngas has no significant effect on the CO conversion. The selectivity to higher alcohols versus methanol is, however, reduced by the presence of CO_2. Therefore CO_2 removal is necessary for processes using sulfide catalysts. Moreover, the sulfide catalysts also are very good water–gas-shift catalysts and produce a large amount of carbon dioxide and hydrocarbons.

3.8. Copper–cobalt catalysts

The modified Fischer–Tropsch catalyst (MFTC) was a homogeneous mixed-oxide formulation containing Cu and Co on an alumina support. Both copper and cobalt are required for higher alcohol synthesis and metallic cobalt should be presented either pure or alloyed with copper. In the MFTC process the various roles of copper are to provide active sites for methanol synthesis, to activate cobalt reduction, and possibly to modify the cobalt by alloying. Indeed, they reported the Co–Cu based catalysts prepared by the citric acid method or by co-precipitation of metal nitrates with an appropriate basic element [9,70]. A representative precursor was described by the following formula: Cu–Co–Cr (Al) $_{0.8}$ $K_{0.09}O_x$ (atomic ratio). MFTC emphasized that the composition of Al < Cu/Co < 3 and Co/Cr > 0.5 is most suitable for the synthesis of higher alcohols from syngas [9]. In some cases potassium can be replaced by Li or Na, and Fe, V, Mn can be substituted for Cr with incorporation of Zn. After calcinations, the precursor was incompletely transformed to the spinel structure with general formula: AB_2O_4 (A=M^{2+} and B=M^{3+}) while sometimes CuO segregates. The Cr^{3+} or $A1^{5+}$ (in the rich-Co catalyst) is usually found as the M^{3+} ion in the spinel structure, while Co^{2+} (Zn^{2+}) and sometimes Cu^{2+} may act as the M^{2+} ion in the spinel though the formation of Cu-spinel which is very difficult, with the exception of samples calcined at a high temperature. Before testing the catalyst was activated under a blend of hydrogen in an inert gas at appropriate temperature. The reduced sample contains both copper and cobalt in metallic form. An intimate mixture of Co and Cu in the final

Table 12
Selected modified Fischer–Tropsch catalysts employed in the direct conversion of syngas to ethanol and mixed alcohols.

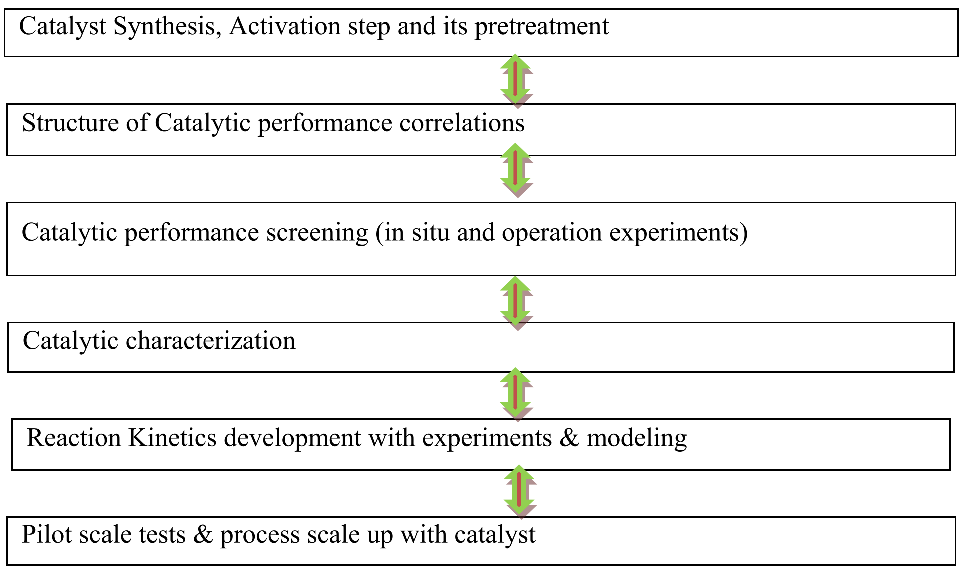
Catalyst	Experimental conditions					
	Temperature (°C)	Pressure (psig)	GHSV (h^{-1})	H_2/CO	X_{CO} (%)	Ref.
Co–Re–Sr/SiO_2	250	300	2000	2.0	4.9	[91]
Fe/Al_2O_3	200	116	40,000	2.0	< 1.0	[91]
Co–Re–Sr/SiO_2	250	305	2000	2.0	5.0	[91]
Co–Ru–Sr/SiO_2	250	305	2000	2.0	4.5	[91]
Co–Ir–Sr/SiO_2	220	305	2000	2.0	2.2	[91]
$KLaCo_{0.7}Cu_{0.3}O_3$	275	1000	5000	2.0	NA	[91]
Co/SiO_2	230	145	4000	2.0	66.2	[45]
Co/Al_2O_3	230	145	4000	2.0	54.6	
Co/MONT (zeolite)	230	145	4000	2.0	57.9	
Co/USY (acid form zeolites)	230	145	4000	2.0	49.2	
Co/ZSM-5	230	145	4000	2.0	21.1	
Co/MCM-22 (30)	230	145	4000	2.0	66.4	
Co/MCM-22 (50)	230	145	4000	2.0	67.6	
Co/DeMCM-22 (80)	230	145	4000	2.0	73.5	
Co/NaMCM-22	230	145	4000	2.0	60.6	
CuO–ZnO–Al_2O_3/ZSM-5	400	574	3500	2.0	53.91	[70]
CuO–ZnO/ZSM-5	400	574	3500	2.0	61.72	
CuO-SiO_2/ZSM-5	400	574	3500	2.0	39.79	
Cr_2O_3–ZnO (Cr/Zn) 2.0)/ZSM-5	400	574	3500	2.0	62.91	
10% Co on mesoporous silica	265	100	NA	2.0	2.6	[100]
15% Co on mesoporous silica	265	100	NA	2.0	11.3	
20% Co on mesoporous silica	265	100	NA	2.0	13.4	

catalyst may be preserved as a result of the careful reduction and thermal decomposition of the spinel form. This is due to the strong interaction within the hydrate cite-like structure (before calcinations) and within spinel (after calcinations) that gives rise to the formation of small cobalt metal crystallites after calcinations [9]. Thus, this prevents sintering of small Co metal particles. In order to avoid the sintering of metal particles, the tailoring reduction of cobalt is one of the bottleneck steps. A slow reduction of Co results in finely dispersed metals and furthermore increases the probability of forming a Cu–Co alloy instead of cobalt crystallites alone. The study of temperature program reduction (TPR) with the help of hydrogen, of Al–Cr–Cu supported Co catalysts indicated that a large proportion of the Co ions in the aluminates and/or chromites is reduced at a lower temperature, but the cobalt reducibility is not affected by the copper content. This could be logically explained by the fact that copper reduced at a low temperature acts a catalyst for cobalt reduction by providing activated hydrogen simultaneously. Cobalt dispersion is improved by copper promotion (the average diameter of particles is always less than 5 nm, even for totally reduced samples) [9]. The improvement of metallic cobalt dispersion is due to the random distribution of cobalt in the spinel type precursor. In essence, under hydrogen reduction and surface reconstruction upon syngas, the spinel phase is probably depleted of its reducible metals which are converted to well-dispersed clusters with depleted mixed oxide support. Additionally, Cr_2O_3 and/or Al_2O_3 promote the synthesis of methanol and stabilize the small copper crystallites as low temperature methanol catalysts. Modified Fischer–Tropsch catalyst (MFTC) strongly underscored the role of copper in higher alcohol synthesis catalyst and the preparative method to produce a homogeneous distribution of cobalt and copper sites. In this case, a Co–Cu alloy was proposed as active component for formation of high alcohols. Indeed, copper is a major component for methanol synthesis and its main function is the dissociative chemisorption of hydrogen and the associative adsorption of CO. Cobalt, an element frequently employed in Fischer–Tropsch synthesis, has the function of dissociative CO adsorption (C–C chain growth) and hydrogenation [9]. The metallic Co sites act as centers for CO dissociation, C–C chain propagation and hydrogenation while the copper sites adsorb CO molecularly via surface migration over a short distance, the adsorbed CO molecule moves to an adsorbed alkyl group and inserts into the bond between the metal site and the alkyl group. Therefore, this insertion is facilitated if the Co and Cu sites are very proximate to each other (a close distance of a few Angstroms) to permit the surface migration of CO adsorbed species as shown in Table 12 with prominent result taking place at different temperature and pressure.

Herein, the main role of copper is to eliminate the activity of cobalt for the formation of hydrocarbons. In other words, the copper component is required to catalyze the initial reduction of cobalt ions and/or to maintain cobalt in the optimum state of reduction. These authors also proposed that the high activity and selectivity of the co-precipitated Cu/Co/ZnO/Al_2O_3 catalysts could result from carbon monoxide being dissociated, but not easily hydrogenated to a stable hydrocarbon, on a Cu/Co cluster and that carbon monoxide insertion occurs by the transfer of an undissociated carbon monoxide molecule from a cobalt ion to an adjacent Cu/Co particle [61,70,94,96,105,9]. As per Institut Francais du Petrole (IFP) Patented catalyst formulations have the following composition on an element basis: 10–50% Cu; 5–25% Co; 5–30% Al; 10–70% Zn; alkali/Al – 0–0.2; Zn/Al=0.4–2.0; Co/Al=0.2–0.75; Cu/Al=0.1–3.0. The homogenous catalysts showed good catalytic performances. The IFP catalyst tests were carried out under 5–15 MPa, T=493–623 K, H_2/CO (ratio)=0.5–4 with small CO_2 also as a reactant and yielded mainly linear primary alcohols following an ASF distribution for carbon chain growth. Under optimal conditions, carbon conversion efficiency of CO and CO_2 is between 5% and 30% and produces a mixture of liquid products containing 30–50% higher alcohols with methane and hydrocarbons being the primary byproducts [9]. IFP catalysts were first commercialized in a pilot plant at Chiba (Japan) for the production of higher alcohols from syngas. However, this plant had been curtailed after operating approximately for 8 months [9]. Several modified IFP catalysts were adjusted by some substitutions or modifications were made, e.g., replacement of Co by other VIII group metals (Fe, Ni), substitution of the alkali elements by other basic components such as alkali-earth. Both the lack of long-term stability and the low activity have limited the commercial application of these

catalysts. The catalyst lifetime has been kept as long as 8000 h at the pilot-scale with little deactivation caused mainly by coke formation and sintering that decreases the homogeneity of the catalyst [110]. This shortcoming could be overcome by an addition of noble metals, especially Rh, which could significantly improve the long-term performance and the selectivity of the catalysts toward higher alcohols.

4. Schematic presentation of principal stages to approach design of new heterogonous catalyst [131–162]



4.1. Types of cobalt Catalysts and methods of deposition of active phase

4.1.1. Impregnations

Cobalt-supported catalysts for FT synthesis are very often prepared by impregnation. Impregnation is a method of cobalt deposition on porous support in which a dry support is contacted with a solution containing dissolved cobalt precursors [152,155,158].

4.1.1.1. Impregnation using solutions of cobalt salts. Incipient wetness impregnation is the most common method to prepare cobalt-supported catalysts. In the incipient impregnation method a solution of cobalt salt, typically cobalt–nitrate, this is contacted with a dry porous support. After being contacted, the solution is aspired by the capillary forces inside the pores of the support. The incipient wetness occurs when all pores of the support are filled with the liquid and there is no excess moisture over and above the liquid required to fill the pores. Although at the first sight the practical execution of incipient wetness impregnation is simple, the fundamental phenomena underlying impregnation and drying are extremely complex. Reproducible synthesis of cobalt catalyst requires careful control of all impregnation parameters: temperature and time of support drying, rate of addition of impregnating solution, temperature and time of drying, etc. Slurry (wet) impregnation represents another technique of introduction of cobalt phase to the catalyst supports. Slurry impregnation entails use of an amount of impregnating liquid in excess of what can be accommodated by the total pore volume of selected porous support. The support is usually added to the impregnating solution heated at 333–363 K to yield slurry [82,83]. The slurry is stirred continuously during impregnation. After removal of the excess liquid phase, the catalyst is dried at sub-atmospheric pressure or in flow of air. The initial drying at sub-atmospheric water is essential to inhibit diffusion of active component to the outer surface of catalyst grains. By applying the ultrasound effect from lower (180 W) to higher (210 W) dosing pattern lower BET surface area of the catalyst obtained whereas highly and evenly distributed smaller cobalt crystallites over the support as reported by Xiaofeng et al. [153]. The textural properties and the size of the cobalt particles change during higher power ultrasound (210 W), and the same phenomenon is also obtained by Liang et al. [150,151,153,154,155]. By implementing the effects of high frequency electromagnetic fields, typically microwaves, or the cavitational energy associated with sonochemistry along with other extreme conditions such as plasmas, high pressure and UV, many researcher groups are synthesizing catalyst batches through these techniques of recent development. In addition they enhanced the energy utilization process with an improved matter of transportation, which provides a novel mixing of technologies by these microwave techniques [150,151,155].

4.1.2. Co-precipitation method

The co-precipitation method has been commonly used for preparation of iron FT catalysts, while for cobalt-supported catalysts very few papers have been published. The precipitation method to prepare cobalt-based catalysts has been employed by many research groups, especially to synthesize inorganic nanoparticles different methods can be adopted [84]. The precipitation of metals from aqueous or non-aqueous solutions typically requires the chemical reduction of a metal cation can be obtained by (a) co-precipitation synthetic methods, (b) synthesis of metals from aqueous solutions, (c) precipitation of metals by reduction from non-aqueous solutions, (d) precipitation of metals by electrochemical reduction, (e) precipitation of metals by radiation-assisted reduction, (f) precipitation of metals by decomposition of

metal organic precursors, (g) precipitation of oxides from aqueous solutions, (h) precipitation of oxides from non-aqueous solutions, (i) co-precipitation of metal chlorides by reactions of molecular precursors, (j) microwave-assisted co-precipitation, (k) sonication-assisted co-precipitation [85].

4.1.3. Deposition precipitation method

The deposition–precipitation method is based on precipitation combined with deposition from a liquid medium. The method combines all the advantages of the precipitation method related to control of the size and size distribution of precipitated particles but diminishes the risk of formation of bulk mixed compounds of support and active phase [82]. With this technique a solvated metal precursor is deposited exclusively onto the surface of a suspended support by slow and homogeneous introduction of a precipitating agent generally hydroxyl ions, in such a way as to avoid nucleation of a solid precursor compound in the bulk solution. The most important issue in this method is to prevent precipitation far from the support surface. Generally, hydrolysis of urea at 323–373 K is used to achieve a slow and homogeneous increase in pH. The process consists of two steps:

(1) precipitation from the bulk solution both in support pores and over support and
(2) Interaction of the precipitate with the support surface.

A fine and homogeneous phase can be obtained by involving surface OH groups of the support in the precipitation process. In the deposition process, adsorption of the metal ions onto the support coincides with nucleation and growth of a surface compound. The support surface acts as a nucleating agent [84].

4.1.4. The Pechini method

In 1967, Pechini developed a modified sol–gel process for metals that are not suitable for traditional sol–gel type reactions due to their unfavorable hydrolysis equilibrium. Although Pechini's original method was developed specifically for the preparation of thin films, it was later adapted to the synthesis of powdered products. The Pechini method, as it is now referred to, relies on the formation of complexes of alkali metals, alkaline earths, transition metals, or even nonmetals with bi- and tridendate organic chelating agents such as citric acid. A polyalcohol such as ethylene glycol is added to establish linkages between the chelates by a poly-esterification reaction, resulting in gelation of the reaction mixture. After drying, the gel is heated to initiate pyrolysis of the organic species, resulting in agglomerated submicron oxide particles [85]. The advantage of the Pechini method lies in the elimination of the requirement that the metals involved form suitable hydroxo complexes. Chelating agents tend to form stable complexes with a variety of metals over fairly wide pH ranges, allowing for the relatively easy synthesis of oxides of considerable complexity.

4.1.5. Sol gel method

Sol–gel is another technique to prepare catalysts for FT synthesis. The sol–gel process also allows mastering and adjusting the surface area, porosity, and particle size of prepared catalysts [84,85]. Although the sol–gel method has been known one of the easiest ways to obtain uniform structure, the microscopic feature strongly depends on the preparation method. The required amount of Co. $(NO_3)_2 \cdot 6H_2O$ was dissolved in ethylene glycol, tetra-ethylortho silicate was added to the solution, and the mixture was heated under vigorous stirring to form a homogeneous solution. Pore size modifiers, such as *N*, *N*-dimethylformamide, and polyethylene glycol (average molecular weight 2000), were added to the solution at that stage. Distilled water and ethanol were then added to the solution dropwise at room temperature, resulting in a homogeneous clear sol. The sol was slowly hydrolyzed by heating at a temperature higher than 353 K for more than 40 h to form a glassy transparent gel. The gel was dried and calcined in nitrogen and air flow at 823 K for 15 h and then reduced in hydrogen flow at 773 K for 15 h. After reduction, transmission electron microscopy displayed a uniform distribution of Co metal particles of 3–5 nm diameters. XPS depth profile analysis of the sol–gel catalysts indicated that the Co concentration was uniform in three dimensions. The sol gel method proved to be more suitable for uniform preparation of highly loaded catalysts (about 60 wt%) than impregnation [84,85,87].

4.1.6. Eggshell catalysts

In recent years, many studies have been concerned with control of the metal profile in support particles. The choice of the optimal catalyst profile in the support is determined by the required activity, selectivity, and other characteristics of the chemical reaction (kinetics, mass transfer). Eggshell catalysts are advantageous in the case of fast reactions with strong diffusion restrictions because the active component is concentrated close to the external pellet surface. Eggshell catalysts have been proposed to overcome difficulties due to diffusion limitations in catalyst pellets in fixed bed FT reactors. It was suggested that smaller than 0.2 mm pellets were required to avoid mass-transport restrictions [82]. Such small catalyst particles would lead to a very significant pressure drop in large commercial fixed bed reactors. Eggshell catalyst pellets of 2 mm diameter introduce design flexibility by decoupling the characteristic diffusion distance in catalyst pellets from pressure drop and other reactor constraints.

4.1.7. Monolithic catalysts

One of the largest advantages of monolithic catalysts is a low pressure drop in a large-scale reactor because of thin catalyst layers with a tunable thickness [86]. Thin catalyst layers also eliminate effects of diffusion limitations. Heat generated by FT reaction can be removed in monolithic catalysts by recycling liquid through the channels of the monolith and an external heat exchanger. Tailoring the layer thickness allows design of monolithic catalysts with optimal activity and selectivity in FT synthesis. No wax–catalyst separation is necessary in monolithic reactors [87].

Two research groups have been working in the area of monolithic catalysts for FT reaction. Three types of monolith are generally used: cordierite, α-Al_2O_3 and steel monoliths (i.e., steel sheets). These monolithic catalysts consist of long parallel channels separated by thin walls [88]. The walls can be either made of cordierite on which a high surface area catalyst support can be wash coated or a suitable catalyst support such as alumina and silica. Different coating thicknesses could be achieved by repeating the coating process. Cobalt active phase in monolith catalysts is deposited by either aqueous co-impregnation [87] or homogeneous deposition precipitation from an aqueous solution of cobalt nitrate and urea. An overall cobalt loading of 10–20 wt% can be obtained.

4.1.8. Colloidal, microemulsion, and solvated metal atom dispersion methods

4.1.8.1. Colloidal method. Colloidal synthesis has been widely as an efficient route to control metal particle size and shape, crystallinity, and crystal structure. Metal colloids displayed remarkable catalytic performance in a wide range of reactions. Stabilization of colloidal systems is a crucial issue in the synthesis of metal colloids and colloid based supported catalysts. Although colloids encapsulated in polymer matrix are very stable, it is not economical and convenient to recover them from the polymer by conventional methods. In addition, metal

sites in a colloidal particle, which is included in polymer, could be inaccessible for reacting molecules [82].

4.1.8.2. Microemulsion method. A considerable number of reports have recently addressed the microemulsion method for preparation of metal-supported catalysts. Microemulsion synthetic methods implemented when a reverse micelle solution contains a dissolved metal salt and a second reverse micelle solution containing a suitable reducing agent is added, the metal cations can be reduced to the metallic state [85]. Synthesis of alloys by reduction, metal oxide formation and other inorganic nano-particles are easy to synthesize using micro-emulsion method. The method usually involves micro-emulsion stabilizer. A stabilizer (emulsifier) is a molecule that possesses both polar and nonpolar moieties. In diluted water (or oil) solution, emulsifier dissolves; it is present in the form of monomer. When the concentration of emulsifier exceeds the critical micelle concentration, the molecules of emulsifier associate spontaneously to form aggregates-micelles. Formation of oil in-water (o/w) or water-in-oil (w/o) reverse micelles could be driven by hydrophobic or hydrophilic interactions of the hydrophobic tail or hydrophilic polar group, respectively. Because microemulsions typically have droplet diameters much smaller than the wavelength of visible light, they can be characterized visually by formation of an optically transparent single phase [82]. A particle size in the range of 5–50 nm depends on the size of microemulsion droplets and can be controlled by adjusting the water to surfactant ratio or concentration of reagents. The metal particles produced by this method usually have a spherical shape.

4.1.8.3. The germ-growth method. Lin et al. has developed a variation of the micro-emulsion process in which seed crystals are first precipitated in the micellar cores and subsequently grown by further addition of reactant. The method was developed specifically for the preparation of nano-particulate Co, which tends to form Co_2B when reduced with borohydride in the presence of high concentrations of water. In this modified method, the [water]/[surfactant] ratio was kept low and constant [85]. After small Co seeds were precipitated in the reverse micelle cores, additional micro-emulsions containing aqueous Co_2+ or BH_4 – were added sequentially, and the process could be repeated several times. With each addition of reactant, the Co was preferentially precipitated on the existing Co seeds rather than nucleating as new crystallites. The size of the resulting nano-crystals could be controlled in the range 3.8–8.8 nm with a relatively narrow size distribution. This method should be adaptable to other metals [90].

4.1.8.4. Hydrothermal/solvothermal processing of nanoparticles and nanocomposites. In a sealed vessel (bomb, autoclave, etc.), solvents can be brought to temperatures well above their boiling points by the increase in autogenous pressures resulting from heating. Performing a chemical reaction under such condition is referred to as solvothermal processing, or in the case of water as solvent, it is hydrothermal processing [85]. Some solvothermal processes indeed involve supercritical solvents. Solvothermal processing allows many inorganic materials to be prepared at temperatures substantially below those required by traditional solid-state reactions [87].

4.1.9. Chemical vapor deposition

The conventional chemical vapor deposition (CVD) method is a well-known technique for deposition of metal oxide particles on powdery supports. CVD involves chemical reactions of gaseous reactants on or near the vicinity of a heated substrate surface. This deposition method can provide nano-structured and functionally coated materials with unique structure. The advantages of CVD are due to the uniform distribution of cobalt nanoparticles on catalyst support and possibly a narrow distribution of cobalt particle size. CVD can be performed either in vacuum or in a flow of carrier gas (Ar, He) [82]. After deposition, the precursor is decomposed at higher temperatures, yielding metallic or oxide nanoparticles.

4.1.10. Plasma methods

Application of plasma techniques for preparation of catalysts was initiated in the 1980s, and a few significant results have been reported in many literatures [89]. Below two techniques are discussed based on plasma spraying and glow discharge plasma. A number of FT synthesis studies have been carried out using iron and bimetallic cobalt–iron [90] catalysts in tube-wall reactors (TWR).

Fu et al. has depicted that through dielectric-barrier discharge (DBD) plasma treatment method, it is easy to replace the traditional calcination method and to prepare Co/CNTs catalyst with uniformly dispersed Co particles towards FTS [155]. The Co-based catalysts prepared by DBD plasma are useful to achieve better FTS performance by calcining the catalysts at 200 °C either in argon or air atmosphere. A big advantage associated with DBD plasma treatment is to make the precursor decomposed at lower temperature with less energy in a short period of time. So plasma technique can be proved as an efficient alternative approach for Co-based catalyst preparation for FT synthesis, comparing to the conventional method [155,162].

Similarly Chu et al. [162] have reported about Co-catalyst both with Al and Si support using the glow discharge plasma, where they found an increased Co dispersion using plasma decomposition instead of thermal calcinations. But limited persons have reported for both plasma spraying and glow discharge plasma methods for FT catalyst. This plasma spraying and glow discharge plasma methods are being implemented in order to combine the effects of without excess use of conventional solvents or ionic liquid usage, and for present time it is necessary to adopt advance technologies, but in terms of the minimization of energy and optimization of reaction control both microwave and ultrasound irradiation, have now been proved to be real options for heterogeneous catalyst synthesis [156,159,161,162].

4.1.11. Templated syntheses

This technique involved with heterogeneous nucleation, or seed formation, in which “seed” crystals serve as nucleation sites for further deposition and growth of crystallites, can essentially be considered one of the simpler forms of a templated synthesis [85]. This technique can be used to increase the average particle size of nanoparticles, such as when aqueous Au_3+ is deposited on colloidal Au, or Ag+ is deposited on colloidal Ag, etc. [91].

4.2. Preparation and characterization techniques of FT Catalysts (thermo-chemical process)

During (GTL) CO-hydrogenation process important stages for the preparation of Co, Fe, Cu supported FT catalysts are displayed in Table 13. All these stages include conditioning, modification, and promotion of catalyst support, preparation of different metals like Co, Ni, Fe, Zn, Ru precursors and eventually promoters, followed by deposition of metals and promoters. Decomposition of metal precursor is an important stage in catalyst preparation. The catalytic performance of FT catalysts is finally adjusted during the reactor start up and on-stream during FT reaction stage. The important point is to emphasize that a catalyst for FT synthesis is a result of the whole preparation procedure and each preparation step does matter in attaining the desired and lasting catalytic performance by the art of practice.

After synthesis most important features are to be covered by its physio-chemical characterization to make the catalyst useful and convenient for the desired catalytic process. Catalyst characterization provides important information about the structure of Co, Ni, Fe, Zn, Ru, based FT catalysts and their precursors. Catalyst characterization allows identification of the active sites for FT reaction and reveals possible routes for optimization of catalyst structure. A wide range of physical and chemical techniques has been used. In many cases, catalyst structure could be investigated during different pretreatments and catalytic reaction under in-situ and operation conditions. Through a critical analysis mentioned below addresses the advances, challenges and uncertainties of catalyst characterization [84,131–144]. Different catalyst characterization techniques which are useful for heterogenous catalyst are (1) optical spectroscopy, (2) UV–visible spectroscopy, (3) FTIR spectroscopy, (4) Raman spectroscopy, (5) diffraction methods like (i) ex-situ characterization of cobalt phases and catalytic supports, (ii) in-situ XRD catalyst characterization, (6) X-ray photoelectron spectroscopy, (7) X-ray absorption spectroscopy (XANES and EXAFS), (8) temperature-programmed reduction, (9) magnetic methods, (10) analytical electron microscopy (a) transmission electron (TEM), (b) scanning electron (SEM), (c) scanning transmission electron (STEM), (d) scanning tunneling electron (STM) microscopes, (11) chemi-sorption methods, (a) hydrogen chemisorption, (b) carbon monoxide chemi-sorption, (c) propene chemisorption [131–162]. Tables 13 and 14 depict more about the different preparation and its characterization techniques which are most crucial steps to be followed.

5. Critical discussion

The following conclusions can be derived from this review on the conversion of syngas to ethanol and higher alcohols: (a) Catalytic conversion of syngas to ethanol and higher alcohols has been studied for the past 90 years using homogeneous and heterogeneous catalysts, but none of the processes have been commercialized, although a few have gone to pilot scale. (b) Higher selectivity to ethanol could be achieved with homogeneous catalysts, but a commercial process based on these catalysts requires extremely high operating pressures, complex catalyst recovery, and expensive catalysts, making their commercial application almost impractical. (c) Rh-based heterogeneous catalysts promoted by Fe or Mn preferentially produce ethanol over other alcohols; the limited availability and high cost of Rh, and the insufficient ethanol yield, can make these catalysts unattractive for commercial application. (d) Modified methanol synthesis and

Table 13
Principal stages in the preparation of metal-supported FT heterogonous catalysts.

Conditioning, Modification and Promotion of catalyst support

⇕

Preparation of cobalt / Iron, precursors and eventually promoters

⇕

Deposition of Cobalt / Iron and promoters on catalyst support

⇕

Decomposition of metal precursor

⇕

Oxidative or reducing pretreatments (Optional)

⇕

Start up of FT reaction and modification of used catalyst in syngas for Liquid hydrocarbons

Table 14
Different characterization technique implemented for FTS catalyst.

Characterization technique	Information gathering about FT catalysts	Ref.
1.Optical spectroscopy	Metal ions (Co, Ni, Fe, Zn, Ru) coordination in its metal precursors and its oxidation stages.	[68]
(UV–visible spectroscopy) (FTIR spectroscopy)	Support identification for (Co, Ni, Fe, Zn, Ru) metal oxides, characterization of metal surface sites using adsorption of molecular probes.	[66,134]
(Raman spectroscopy)	Characterization of metal oxide species.	[61,63–65]
2. Diffraction methods	Identification of different metal oxidized and reduced crystalline phases measuring extent of FTS metal reduction.	[65,135,137]
	Measuring sizes of metal crystallites characterization of the structure of catalyst supports (Al_2O_3, TiO_2, SBA-15, MCM-41, etc.). Detection of hydrocarbon built up in the catalysts.	[138,139,142,152,155,158]
3. X-ray photoelectron spectroscopy	Identification of metal oxidized and reduced phases. Measuring suitable metal particle size (catalysts with low cobalt contents).	[66,84,86]
	Evaluating extent of metal like Co, Cu, Fe, reduction.	[107,134]
4. X-ray absorption Spectroscopy	Identification of cobalt oxidized and reduced crystalline and amorphous phase detection of bimetallic clusters. Detection of bimetallic clusters. Reduced finger prints of catalysts.	[84,86]
5.Temperature-programmed reduction	Detection of easily and hardly reducible cobalt phases. Evaluation of cobalt reducibility and fraction of cobalt metal phase. Measuring metal like Co, Cu, Fe, Al, particle size.	[61,63,64,137,138,152]
6. Magnetic methods	Measuring size and morphology of metal particles.	[139,140,143–145]
7. Analytic electron microscopy and related techniques	Characterization of support structure qualitative evaluation of the fraction of metal oxide phases and Co, Cu, Fe, K, Al, Si support amorphous compounds, information about localization of cobalt and promoter.	[65,82,86,107,135,136]
8. Chemisorption methods	Number and type of active metal surface sites.	[139,140,146–149]

Fischer–Tropsch synthesis catalysts based on CuZn, CuCo, and MoS_2 have been evaluated in syngas conversion to mixed alcohols, and some of them have been used in pilot plant testing. The rates of ethanol and total alcohol production are significantly lower than those achieved in methanol synthesis (1300–1500 mg methanol/(g. cat. h)). Thus, significant improvements in the alcohol production rate must be achieved. (e) Direct synthesis of ethanol and higher alcohols from syngas is thermodynamically feasible, but kinetically controlled. (f) The linear homologation of C_1–C_2 alcohol is the bottleneck in ethanol and HAS. Methanol homologation, by co-feeding either methanol or formaldehyde along with syngas over a suitably modified catalyst composition, appears to be a promising approach to produce ethanol with high yields and selectivity.

5.1. Catalyst selection/development

Catalytic synthesis of ethanol from syngas suffers from low yield and poor selectivity of the desired alcohol product due to the slow kinetics of the C_1–C_2 linear chain growth and fast chain growth to form C_2+alcohols. R&D work to improve the ethanol yield and selectivity should focus on developing a methodology for increasing the kinetics of the C_1–C_2 chain growth. Substantial research, as evidenced by countless journal articles, has been carried out on developing direct ethanol synthesis, HAS, and methanol homologation catalysts over the past 90 years or so. In this section, we identify the best catalyst candidates from past research and development that merit further research and development for ethanol and HAS. Homogeneous catalysts based on noble metals may be rejected from further consideration because of the high cost of the noble metal catalysts and the difficulties associated with catalyst recovery and reuse. Some of the best-performing heterogeneous catalysts and reaction operating conditions and its proper characterizations for morphology study as well as composition, bond energy involved are discussed in this review, further depicted in Tables 13 and 14. Among them, the low yield combined with high cost and limited availability of Rh is sufficient to eliminate Rh-based catalysts from further consideration also, unless an extremely active catalyst containing a very small amount of Rh (e.g., 0.1 wt%) and/or a novel process that improves the ethanol yield are developed. Furthermore, the high-temperature K_2O–Pd–ZrO_2–ZnO–MnO catalyst that uses severe operating conditions (high temperature and very high pressure) may also be eliminated from consideration because of the following factors: (1) its high operating pressure is not compatible with the operating pressure envisioned for commercial and developmental biomass gasifiers. (2) Its high operating temperature results in high selectivity for methane and isobutanol, but not for ethanol. The above concerns leave the following classes of heterogeneous catalysts for further consideration: (a) alkali-modified, low-temperature methanol synthesis catalysts based on Cu–ZnO/Al_2O_3, (b) alkali-modified CuCo-based modified FT catalysts, (c) alkali-modified MoS_2-based catalysts, (d) It is noteworthy that formulations based on these three classes of catalysts have been used in pilot plants for HAS or are being considered as potential catalyst candidates for pilot plants to be constructed in the future. Among the three classes, the Cu–ZnO/Al_2O_3 catalyst shows the lowest ethanol yield but is highly selective toward alcohols compared to hydrocarbons, whereas the CuCo-based IFP catalysts exhibit a high ethanol yield but with lower selectivity. The MoS_2-based catalysts show relatively higher ethanol selectivity, but still lower ethanol yield. Modifications need to be made to these baseline catalyst formulations to improve the yield and selectivity toward ethanol. Promoters that could be considered include (1) alkali metal to be used and its concentration in the catalyst and (2) the way promoters are loaded. K and Cs are the promoters commonly used as alkali promoters in these catalytic systems, and both have shown to improve the ethanol yield and selectivity. While a low concentration (around or lower than 3 wt%) of alkali is sufficient in Cu-based methanol synthesis catalysts, the MoS_2 based catalyst may require a higher alkali loading, even up to 20 wt%. Hence, the concentration of alkali required for the given type of catalyst needs to be optimized. In addition to alkali promoters, Group VII and Group VIII metals can also be used as a promoter to increase the activity, thereby increasing the ethanol yield. For example, Co and Pd additions have been shown to increase the rate of methanol homologation to ethanol. Methanol can be added to the feed via the recycling of a portion of the methanol in a commercial embodiment, or methanol that is formed in-situ can undergo both homologation and coupling reactions to produce ethanol. Mn is a known promoter for enhancing the production of ethanol and also significantly promotes ethylene formation, which can be hydrated to form ethanol by the known ethylene hydration process over a solid acid catalyst. The Co to Mo ratio has been shown to be an important parameter for both unsulfided and sulfided Co–Mo-based catalysts, with an optimum for alcohol production of 1 to 7. High dispersion of the catalyst that has been shown to improve activity for HAS and is also a very important consideration in catalyst development. Catalysts containing nanoparticles of active metals should be prepared with high dispersion and with structural promoters to prevent sintering at reaction conditions. Catalyst preparation techniques will include impregnation and precipitation, procedures specifically designed to yield nanoparticles of the metals with high dispersion, such as deposition–precipitation using a special precipitating agent. Scalability and cost of catalyst preparation/modification is also an important consideration. Exotic methods of catalyst modification/preparation that cannot be easily scaled up using conventional commercial equipment should be avoided. Although methanol homologation via reductive carbonylation reactions seems promising, suitable catalysts having multiple functions are required to improve the conversion and selectivity to ethanol.

6. Summary and future outlook

Before CO-hydrogenation, prior most work is to strengthen catalyst synthesis, catalysts characterization, and evaluation of catalytic performance are the primary and probably most important stages in the design of any FTS catalysts. Meanwhile different catalyst synthesis routes, promotion with noble metals and metal oxides, catalyst pretreatments, and support effects, provide the efficient tools to control the structure, chemical, physical, and mechanical properties of FTS catalysts. The bulk and surface structure of any FTS supported catalysts could be identified by a wide range of characterization techniques. Syngas can be converted to ethanol directly using Rh-based catalysts; however, the Rh is very expensive, its availability is limited, and the yield is insufficient to justify its use. HAS, resulting in a mixture of C_1–C_5 alcohols, is a more desirable route, particularly when coupled with methanol homologation to increase the ethanol yield. HAS and methanol homologation catalysts are similar and consist of a combination of alkali promoted base metals (e.g., Cu, Zn, Co, and Mo) on oxide supports. Catalysts of particular interest for further improvement include Cu–Co, un-sulfided Co–Mo, and un-promoted and cobalt promoted MoS_2. Current total alcohol yields from these catalysts are in the range between 100 and 600 g/(kg.cat. h), as compared to the benchmark 1300–1500 g/(kg. cat. h) methanol yield typically obtained in the commercially practiced methanol synthesis process. Also, hydrocarbons, especially methane, and CO_2 are produced, thereby reducing total alcohol and ethanol selectivities. The major technical challenge is to produce an ethanol-rich HAS product from

biomass- and/or coal-derived syngas that will be cost competitive with corn-or petroleum-based ethanol. A systematic experimental process development and process integration study is needed to optimize ethanol synthesis from syngas and to efficiently integrate the synthesis and separation steps into an overall indirect liquefaction plant involving gasification, syngas cleanup, and syngas conversion. To carry out experiments in a fixed bed reactor with plug flow hydrodynamics like Jr. BTRS high pressure and optimized temperature range, which operates in the kinetic regime and in the isothermal mode at (H_2/CO) 1–2 and 1–5 MPa of total pressure probably provides the most suitable methodology for preliminary evaluation of the performance of FTS catalysts. To attain a high and stable yield of long chain hydrocarbons like olifines, paraffins, aromatics, FTS catalysts should have an optimal density of Co, Fe, Cu, metal active sites. The active metal component should be used very efficiently; loss of cobalt in the support matrix should be avoided. The catalyst should exhibit high stability during FT synthesis. The cost of the catalyst should be moderate to allow possible industrial utilization for commercialization. Thus, the first objective of any catalyst preparation is to generate the optimal number of active sites. It has been largely accepted that FT synthesis proceeds on cobalt metal particles. Thus, the goal of FT catalyst preparation is to generate a significant concentration of stable FTS metal surface sites. The number of FTS metal sites depends on the size of cobalt particles and their reducibility. An optimal equilibrium between FTS catalyst dispersion and reducibility can be obtained using different catalytic supports, like methods of cobalt deposition, pretreatments, and promotion with noble metals and metal oxides. There is generally a consensus in the literature that the FT reaction is not structure sensitive at least for cobalt larger particles (size $>$ 6 nm). Several methods of deposition of the active phase probably, could generate very small cobalt particles ($<$ 4–6 nm), the catalysts containing these very small particles do not normally exhibit adequate catalytic performance due to their unstable position, as there could be chance of deoxidizition, sintering, carburizing, and reaction with support structure, which leads to formation FTS catalyst and support mixed oxides. Second, when particles are very small, their electronic, magnetic, optical, and adsorption properties could be dramatically altered, due to its quantum size effect. The quantum size effect on the structure of metal and oxide particles is usually observed when the particle is getting smaller than 10 nm and its entire tendency gradually increases as metal size approaches towards 3–4 nm. In addition to the overall number, repartition of cobalt surface sites in a catalyst grain could be essential in attaining a high yield of hydrocarbons. In fixed bed tubular reactors, mainly involving catalyst particles in between 1 and 3 mm, diffusion of reagents, intermediates, and final products could be relatively slow and affect the FT reaction rate and selectivity. The methods of eggshell catalyst synthesis many times seem to provide optimized and efficient FTS catalyst like cobalt catalysts for fixed bed reactor operation. Cobalt and copper oxide could react with most oxide supports yielding Co, Cu support mixed compounds. Those compounds are difficult to reduce at moderate reduction temperatures and unable to provide any active sites for FT synthesis. Production of undesired mixed compounds could be minimized by adjusting the parameters of catalyst synthesis and pretreatment techniques. Many papers depict that the performance of FT catalysts evolves with time on-stream. Several days and weeks may be required to attain the steady-state conditions even in a laboratory-scale, pilot scale-up reactor. Significant modifications of catalyst structure could occur during the FT reactor start up and on-stream during FT synthesis. These modifications could be related to different phenomena like exothermic nature of the reaction, temperature control, impurities in the feed gases, and presence of water, carbon dioxide, heavier hydrocarbons, and organic compounds in the reaction products. Catalyst attrition could also be one of the probable reasons, which drop down catalytic performance in a slurry reactor. It is necessity of time to understand and control the phenomena that occur in the FTS catalyst during FT reaction for better yield and selectivity as well to represent a significant challenge. Catalyst modifications under the influence of the FT reaction medium seem to be the most obscure area in designing of FTS catalysts. Because of the relatively low space velocities, a significant amount of catalyst is required for a slurry bubble column and fixed bed multi-tubular reactor. This involves the requirement to the catalyst cost; again promotion even with small amounts of noble metal addition using sophisticated methods of FTS catalyst preparation could significantly increase the cost of cobalt FT catalysts and overall technology.

Acknowledgments

One of the authors Dr. Sahu likes to thank University of Malaya, Ministry of Higher Education, Malaysia, High Impact Research (UM.C/HIR/MOHE/ENG/20). The financial support provided by Department of Science and Technology, Government. of India, is gratefully acknowledged by P. Mohanty and K. K. Pant.

References

[1] Rofer-De-Poorter CK. A comprehensive mechanism for the Fischer–Tropsch synthesis. Chem Rev 1981;81:447–74.
[2] Spivey JJ, Dooley KM, editors. Catalysis, a review of recent literature, catalysis, specialist periodical reports, 19. Cambridge: The Royal Society of Chemistry; 2006.
[3] Martinez A, Rollan J, Arribas MA, Cerqueira HS, Costa AF, Aguiar EFS. A detailed study of the activity and deactivation of zeolites in hybrid Co/SiO_2-zeolite Fischer–Tropsch catalysts. J Catal 2007;249:162–73.
[4] Adesina AA. Hydrocarbon synthesis via Fischer–Tropsch reaction: travails and triumphs. Appl Catal A 1996;138:345–67.
[5] Seddon D. Reformulated gasoline, opportunities for new catalyst technology. Catal Today 1992;15:1–21.
[6] Nagineni VS, Zhao S, Potluri A, Liang Y, Siriwardane U, Seetala NV, Fang J, Palmer J, Kuila D. Microreactors for syngas conversion to higher alkanes: characterization of sol–gel-encapsulated nanoscale Fe–Co catalysts in the microchannels. Ind Eng Chem Res 2005;44:5602–7.
[7] Khodakov AY. Fischer–Tropsch synthesis: relations between structure of cobalt catalysts and their catalytic performance. Catal Today 2009;144: 251–7.
[8] Laan GPV, Beenackers AACM. Kinetics and selectivity of the Fischer – Tropsch synthesis: a literature review. Catal Rev – Sci Eng 1999;41(3–4):255–318.
[9] Xiaoding X, Doesburg EBM, Scholten JJF. Synthesis of higher alcohols from syngas – recently patented catalysts and tentative ideas on the mechanism. Catal Today 1987;2:125–70.
[10] Brady RC, Pettit R. Mechanism of the Fischer–Tropsch reaction. The chain propagation step. J Am Chem Soc 1981;103(5):1287–9.
[11] 〈http://india.world-ctl.com/〉; [accessed 23.12].
[12] 〈http://www.chemlink.com.au/gtl.htm〉 [accessed 24.12.12].
[13] Friedel RA, Anderson RB. Composition of synthetic liquid fuels. I. Product distribution and analysis of C5–C8 paraffin isomers from cobalt catalyst. J Am Chem Soc 1950;72:1212–5.
[14] Bertole CJ, Kiss G, Mims CA. The effect of surface-active carbon on hydrocarbon selectivity in the cobalt-catalyzed Fischer–Tropsch synthesis. J Catal 2004;223:309–18.
[15] Buchang S, Davis BH. Fischer–Tropsch synthesis: accounting for chain-length related phenomena. Appl Catal A, 277; 2004; 61–9.
[16] Mohanty P, Pant KK, Mittal R. Hydrogen generation from biomass materials: challenges and opportunities. WIREs Energy Environ 2014. http://dx.doi.org/10.1002/wene.111.
[17] Novak S, Madon RJ, Suhl H. Models of hydrocarbon product distributions in Fischer–Tropsch synthesis. J Phys Chem 1981;74(11):6083–91.
[18] Shi B, Davis BH. 13'C-tracer study of the Fischer–Tropsch synthesis: another interpretation. Catal Today 2000;58:255–61.
[19] Madon RJ, Taylor WF. Fischer–Tropsch synthesis on a precipitated iron catalyst. J Catal 1981;69(1):32–43.
[20] Iglesia E, Reyes SC, Madon RJ. Transport-enhanced alpha-olefin readsorption pathways in Ru catalyzed hydrocarbon synthesis. J Catal 1991;129 (1):238–56.
[21] Madom RJ, Iglesia E. The importance of olefin readsorption and H_2/CO reactant ratio for hydrocarbon chain growth on ruthenium catalysts. J Catal 1993;139(2):576–90.
[22] Hardy LI, Gillham RW. Formation of hydrocarbons from the reduction of aqueous CO_2 by zero-valent iron. Environ Sci Technol 1996;30:57–65.

[23] Tien-Thao N, Zahedi-Niaki MH, Alamdari H, Kaliaguine S. Effect of alkali additives over nanocrystalline Co–Cu-based perovskites as catalysts for higher-alcohol synthesis. J Catal 2007;245:348–57.
[24] Komaya T, Bell A. Estimates of rate coefficients for elementary processes occurring during Fischer–Tropsch synthesis over Ru/TiO_2. J Catal 1994;146(1):237–48.
[25] Kuipers EW, Scheper C, Wilson JH, Vinkenburg IH, Oosterbeek H. Non-ASF product distributions due to secondary reactions during Fischer–Tropsch synthesis. J Catal 1996;158(1):288–300.
[26] Dictor RA, Bell AT. An explanation for deviations of Fischer–Tropsch products from a Schuiz–Flory distribution. Ind Eng Chem Res 1983;22(4):678–81.
[27] Bartholomew CH, Pannell RB. The stoichiometry of hydrogen and carbon monoxide chemisorption on alumina- and silica-supported nickel. J Catal 1980;65(2):390–401.
[28] Bridge ME, Comrie CM, Lambert RM. Hydrogen chemisorption and the carbon monoxide–hydrogen interaction on cobalt (0001). J Catal 1979;58(1):28–33.
[29] Christmann K, Schober O, Ertl G, Neumann M. Adsorption of hydrogen on metal single crystal surfaces. J Chem Phys 1974;60(11):4528–40.
[30] Bajusz IG, Goodwin JG. Hydrogen and temperature effects on the coverages and activities of surface intermediates during methanation on Ru/SiO_2. J Catal 1997;169(1):157–65.
[31] Curulla-Ferre D, Govender A, Bromfield TC, Niemantsverdriet JW. A DFT study of the adsorption and dissociation of CO on sulfur-precovered Fe100. J Phys Chem B 2006;110(28):13897–904.
[32] Huang DM, Cao DB, Li YW, Jiao H. Density function theory study of CO adsorption on Fe_3O_4 (111) surface. J Phys Chem B 2006;110(28):13920–5.
[33] Jiang M, Koizumi N, Yamada M. Adsorption properties of iron and iron–manganese catalysts investigated by in-situ diffuse reflectance FTIR spectroscopy. J Phys Chem B 2000;104(32):7636–43.
[34] Bian G, Oonuki A, Kobayashi Y, Koizumi N, Yamada M. Syngas adsorption on precipitated iron catalysts reduced by H2, syngas or CO and on those used for high-pressure FT synthesis by in situ diffuse reflectance FTIR spectroscopy. Appl Catal A 2001;219(1–2):13–24.
[35] Lox ES, Froment GF. Kinetics of the Fischer–Tropsch reaction on a precipitated promoted iron catalyst. 1. Experimental procedure and results,. Ind Eng Chem Res 1993;32(1):61–70.
[36] Shustorovich E, Bell AT. Analysis of CO hydrogenation pathways using the bond-order-conservation method. J Catal 1988;113(2):341–52.
[37] Zhang ZL, Kladi A, Verykios XE. Surface species formed during CO and CO_2 hydrogenation over Rh/TiO_2 (W6+) catalysts investigated by FTIR and mass-spectroscopy. J Catal 1995;156(1):37–50.
[38] Rabo JA, Risch AP, Poutsma ML. Reactions of carbon monoxide and hydrogen on Co, Ni, Ru, and Pd metals. J Catal 1978;53(3):295–311.
[39] McCarty JG, Wise H. Hydrogenation of surface carbon on alumina-supported nickel. J Catal 1979;57(3):406–16.
[40] Rohr F, Lindvag OA, Holmen A, Blekkan EA. Fischer–Tropsch synthesis over cobalt catalysts supported on zirconia-modified alumina. Catal Today 2000;58(4):247–54.
[41] Patel S, Pant KK. Kinetic modeling of oxidative steam reforming of methanol over $Cu/ZnO/CeO_2/Al_2O_3$ catalyst. Appl Catal A 2009;356(2):189–200.
[42] Adam B, Pant KK, Gupta R. Hydrogen production from ethanol by reforming in supercritical water using Ru/Al_2O_3 catalyst. Energy Fuels 2007;21(6):3541–7.
[43] Belambe AR, Oukaci R, Goodwin JG. Effect of pretreatment on the activity of a Ru-promoted Co/Al_2O_3 Fischer–Tropsch catalyst. J Catal 1997;166:8–15.
[44] Froseth V, Storsaeter S, Borg O, Blekkan EA, Ronning M, Holmen A. Steady state isotopic transient kinetic analysis (SSITKA) of CO hydrogenation on different Co catalyst. Appl Catal A Gen 2005;289:10–5.
[45] Ngamcharussrivichai C, Imyim A, Li X, Fujimoto K. Active and selective bifunctional catalyst for gasoline production through a slurry-phase Fischer–Tropsch synthesis. Ind Eng Chem Res 2007;46:6883–90.
[46] Nandini A, Pant KK, Dhingra SC. Characterization and activity of K, CeO_2 and Mn promoted Ni/Al_2O_3 catalysts for carbon dioxide reforming of methane. Ind Eng Chem Res 2006;45:7435–43.
[47] Chang J, Bai L, Teng B, Zhang R, Yang J, Xu Y, Xiang H, Li Y. Kinetic modeling of Fischer–Tropsch synthesis over Fe–Cu–K–SiO_2 catalyst in slurry phase reactor. Chem Eng Sci 2007;62(18–20):4983–91.
[48] Botes FG. Water–gas-shift kinetics in the iron-based low-temperature Fischer–Tropsch synthesis. Appl Catal A 2007;328(2):237–42.
[49] Hayakawa H, Tanaka H, Fujimoto K. Studies on catalytic performance of precipitated iron/silica catalysts for Fischer–Tropsch synthesis. Appl Catal A 2007;328(2):117–23.
[50] Nawdali M, Ahlafi H, Pajonk GM, Bianchi D. Elementary steps involved in the hydrogenation of the linear CO species adsorbed on a Ru/Al_2O_3 catalyst. J Mol Catal A 2000;162(1–2):247–56.
[51] Sanjay P, Pant KK. Hydrogen production by oxidative steam reforming of methanol using cerial promoted cupper alumina catalysis. Fuel Cell Technol 2007;88(8):825–32.
[52] Sahoo DR, Shilpi V, Patel S, Pant KK. Kinetic modeling of steam reforming of ethanol for the production of hydrogen over Co/Al_2O_3 catalyst. Chem Eng J 2007;125:139–47.
[56] Sexton BA, Somoriai GA. The hydrogenation of CO and CO_2 over polycrystalline rhodium: correlation of surface composition, kinetics and product distributions. J Catal 1977;46:167–89.
[57] Ge Q, Neurock M. CO adsorption and dissociation over stepped Co surfaces. J Phys Chem B 2006;110:15368–80.
[58] Gong XQ, Raval R, Hu P. CO dissociation and O removal on Co(0001): a density functional theory study. Surf Sci 2004;562:247–56.
[59] Inderwildi OR, Jenkins SJ, King DA. Fischer–Tropsch mechanism revisited: alternative pathways for the production of higher hydrocarbons from synthesis gas. J Phys Chem C 2008;112:1305–7.
[60] Forzatti P, Tronconi E, Pasquon I. Higher alcohol synthesis. Catal Rev: Sci Eng 1991;33(1–2):109–68.
[61] Mahdavi V, Peyrovi MH, Islami M, Mehr JY. Synthesis of higher alcohols from syngas over Cu–Co_2O_3/ZnO, Al_2O_3 catalyst. Appl Catal A 2005;281:259–65.
[62] Lietti L, Tronconi E, Forzatti P. Mechanistic aspects of the higher alcohol synthesis over K_2O-promoted ZnCr oxide: temperature-programmed reaction and flow experiments of C_3, C_4, and C5 oxygenates. J Catal 1992;135:400–19.
[63] Hilmen AM, Xu M, Gines MJL, Iglesia E. Synthesis of higher alcohols on copper catalysts supported on alkali-promoted basic oxides. Appl Catal A 1998;169:355–72.
[64] Xu M, Gines MJL, Hilmen AM, Stephens BL, Iglesia E. Isobutanol and methanol synthesis on copper catalysts supported on modified magnesium oxide. J Catal 1997;171:130–47.
[65] Hedrick SA, Chuang SSC, Pant A, Dastidar AG. Activity and selectivity of Group VIII, alkali-promoted Mn–Ni, and Mo-based catalysts for C_{2+} oxygenate synthesis from the CO hydrogenation and $CO/H_2/C_2H_4$ reactions. Catal Today 2000;55:247–57.
[66] Matsuzaki T, Hanaoka T, Takeuchi K, Arakawa H, Sugi Y, Wei K, Dong T, Reinikainen M. Oxygenates from syngas over highly dispersed cobalt catalysts. Catal Today 1997;36:311–24.
[67] Mazanec TJ. On the mechanism of higher alcohol formation over metal oxide catalysts: I. A rationale for branching in the synthesis of higher alcohols from syngas. J Catal 1986;98:115–25.
[68] Ponec V. Active centres for synthesis gas reaction. Catal Today 1992;12:227–54.
[69] Hindermann JP, Hutchings GJ, Kiennemann A. Mechanistic aspects of the formation of hydrocarbons and alcohols from CO hydrogenation. Catal Rev: Sci Eng 1993;35:1–27.
[70] Erena J, Arandes JM, Bilbao J, Aguayo AT. Study of physical mixtures of Cr_2O_3-ZnO and ZSM-5 catalysts for the transformation of syngas into liquid hydrocarbons. Ind Eng Chem Res 1998;37:1211–9.
[71] Patel S, Pant KK. Selective production of hydrogen via oxidative steam reforming of methanol using Cu–Zn–Ce–Al oxide catalysts. Chem Eng Sci 2007;62:5436–43.
[72] Steen EV, Helden PV. A DFT study of hydrogen dissociation on CO- and C-precovered Fe(100) surfaces. J Phys Chem C 2010;114(13):5932–40.
[73] Li Z, Fu Y, Jiang M. Structures and performance of Rh–Mo–K/Al_2O_3 catalysts used for mixed alcohol synthesis from synthesis gas. Appl Catal A 1999;187:187–98.
[74] Patel S, Pant KK. Activity and stability enhancement of copper–alumina catalysts using cerium and zinc promoters for the selective production of hydrogen via steam reforming of methanol. J Power Sourc 2006;159:139–143.
[75] Xiang M, Li D, Li W, Zhong B, Sun Y. Potassium and nickel doped β-Mo_2C catalysts for mixed alcohols synthesis via syngas. Catal Commun 2007;8:513–7.
[76] Wender I. Reactions of synthesis gas. Fuel Process Technol 1996;48:189–297.
[77] Klier K, Beretta A, Sun Q, Feeley OAC, Herman RG. Catalytic synthesis of methanol, higher alcohols and ethers. Catal Today 1997;36:3–14.
[78] Herman RG. Advances in catalytic synthesis and utilization of higher alcohols. Catal Today 2000;55:233–45.
[79] Verkerk KAN, Jaeger B, Frinkeldei CH, Keim W. Recent developments in isobutanol synthesis from synthesis gas. Appl Catal A 1999;186:407–31.
[80] Kung HH. Deactivation of methanol synthesis catalysts – a review. Catal Today 1992;11:443–53.
[81] Elliott DJ. Higher alcohol synthesis over CuO/ZnO catalysts: relationship between methanol and higher alcohol synthesis. J Catal 1988;111:445–9.
[82] Tronconi E, Lietti L, Forzatti P, Pasquon I. Higher alcohol synthesis over alkali metal-promoted high-temperature methanol catalysts. Appl Catal 1989;47:317–33.
[83] Tronconi E, Forzatti P, Pasquon I. An investigation of the thermodynamic constraints in higher alcohol synthesis over Cs-promoted ZnCr-oxide catalyst. J Catal 1990;124:376–90.
[84] Hoflund GB, Epling WS, Minahan DM. Reaction and surface characterization study of higher-alcohol synthesis catalysts XII: K- and Pd-promoted Zn/Cr/Mn spinel. Catal Today 1999;52:99–109.
[85] Lin XM, Sorensen CM, Klabunde KJ, Hajipanayis GC. Control of cobalt nanoparticle size by the germ-growth method in inverse micelle system: size dependent magnetic properties. J Mater Res 1999;14:1542–7.
[86] Epling WS, Hoflund GB, Hart WM, Minahan DM. Reaction and surface characterization study of higher alcohol synthesis catalysts. J Catal 1997;172:13–23.
[87] Rajamathi M, Seshadri R. Oxide and chalcogenide nanoparticles from hydrothermal/solvothermal reactions. Curr Opin Solid State Mater Sci 2002;6:337–45.
[88] Epling WS, Hoflund GB, Minahan DM. Higher alcohol synthesis reaction study VI: effect of Cr replacement by Mn on the performance of Cs- and Cs, Pd-promoted Zn/Cr spinel catalysts. Appl Catal A 1999;183:335–43.
[89] Lietti L, Forzatti P, Tronconi E, Pasquon I. Temperature-programmed reaction of C_4 oxygenates on unpromoted and K-promoted ZnCr oxide in relation to the mechanism of the higher alcohol synthesis. J Catal 1990;126:401–20.

[90] Zhang Z, Han M. Template-directed growth from small clusters into uniform silver nanoparticles. Chem Phys Lett 2003;374:91–4.
[91] Subramani V, Gangwal SK. A review of recent literature to search for an efficient catalytic process for the conversion of syngas to ethanol. Energy Fuels 2008;22:814–39.
[92] Tronconi E, Lietti L, Groppi G, Forzatti P, Pasquon I. Mechanistic kinetic treatment of the chain growth process in higher alcohol synthesis over a Cs-promoted Zn–Cr–O catalyst. J Catal 1992;135:99–114.
[93] Patel S, Pant KK. Effect of preparation condition on the characteristics and activity of $Cu/ZnO/CeO_2/Al_2O_3$ catalyst for oxidative steam reforming of methanol. Indian Chem Eng 2008;49:351–61.
[94] Sheffer GR, King TS. Effect of preparation parameters on the catalytic nature of potassium promoted Cu–Co–Cr higher alcohol catalysts. Appl Catal 1988;44:153–64.
[95] Nandini A, Pant KK, Dhingra SC. Deactivation studies on $Ni–K/CeO_2–Al_2O_3$ catalyst for dry reforming of methane. Ind Eng Chem Res 2007;46:1731–6.
[96] Smith KJ, Anderson RB. A chain growth scheme for the higher alcohols synthesis. J Catal 1984;85:428–36.
[97] Majocchi L, Liette L, Beretta A, Forzatti P, Micheli E, Tagliabue L. Synthesis of short chain alcohols over a Cs-promoted $Cu/ZnO/Cr_2O_3$ catalyst. Appl Catal A Gen 1998;166:393–405.
[98] Nunan JG, Bogdan CE, Klier K, Smith KJ, Young CC, Herman RG. Higher alcohol and oxygenate synthesis over cesium-doped Cu/Zno catalysts. J Catal 1989;116:195–221.
[99] Takeuchi K, Matsuzaki T, Arakawa H, Sugi Y. Synthesis of ethanol from syngas over $Co–Re–Sr/SiO_2$ Catalysts. Appl Catal 1985;18:325–34.
[100] Schulz J, Bandermann F. Conversion of ethanol over zeolite H-ZSM-5. Chem Eng Technol 1994;17:179–86.
[101] Vannice MA. The catalytic synthesis of hydrocarbons from H_2/CO mixtures over the Group VIII metals: V. The catalytic behavior of silica-supported metals. J Catal 1977;50:228–36.
[102] Gysling HJ, Monnier JR, Apai G. Synthesis, characterization, and catalytic activity of $La–RhO_3$. J Catal 1987;103:407–18.
[103] Watson PJ, Somorjai GA. The formation of oxygen-containing organic molecules by the hydrogenation of carbon monoxide using a lanthanum rhodate catalyst. J Catal 1982;74:282–95.
[104] Woo HC, Nam I, Lee JS, Chung JS, Kim YG. Structure and distribution of alkali promoter in K/MoS_2 catalysts and their effects on alcohol synthesis from syngas. J Catal 1993;142:672–90.
[105] Bae JW, Park S, Kang S, Lee Y, Jun K, Rhee Y. Effect of Cu content on the bifunctional Fischer Tropsch FeCuK/ZSM-5 catalyst. J Ind Eng Chem 2009;15:798–802.
[106] Tanaka K, Okuhara T. Molecular mechanisms of catalytic isomerization and hydrogen exchange of olefins over the MoS_2 single crystal catalysts: regulation of catalytic processes by the conformation of active sites. J Catal 1982;78:155–64.
[107] Iranmahboob J, Toghiani H, Hill DO. Dispersion of alkali on the surface of $Co-MoS_2$/clay catalyst: a comparison of K and Cs as a promoter for synthesis of alcohol. Appl Catal A: Gen 2003;247:207–18.
[108] Dianis WP. Characterization of metal sulfide Fischer–Tropsch catalysts by temperature programmed desorption. Appl Catal 1987;30:99–121.
[109] Inui T, Kuroda T, Takeguchi T, Miyamoto A. Selective conversion of syngas to alkenes and aromatic-rich gasoline on iron—manganese—ruthenium containing composite catalysts. Appl Catal 1990;61:219–33.
[110] Mirodatos C, Praliaud H, Primet M. Deactivation of nickel-based catalysts during CO methanation and disproportionation. J Catal 1987;107:275–87.
[111] Khodakov AY, Chu W, Fongarland P. Advances in the development of novel cobalt Fischer – Tropsch catalysts for synthesis of long-chain hydrocarbons and clean fuels. Chem Rev 2007;107:1692–744.
[112] Yermakov YI. Organometallic compounds in the preparation of supported catalysts. J Mol Catal 1993;21:35–55.
[113] Okabe K, Li X, Wei M, Arakawa H. Fischer–Tropsch synthesis over $Co–SiO_2$ catalysts prepared by the sol–gel method. Catal Today 2004;89:431–8.
[114] Ernst B, Bensaddik A, Hilaire L, Chaumette P, Kiennemann A. Study on a cobalt silica catalyst during reduction and Fischer–Tropsch reaction: in situ EXAFS compared to XPS and XRD. Catal Today 1998;39:329–41.
[115] Perez-Cadenas AF, Zieverink MMP, Kapteijn F, Moulijn JA. High performance monolithic catalysts for hydrogenation reactions. Catal Today 2005;105:623–8.
[116] Hilmen AM, Bergene E, Lindvag OA, Schanke D, Eri S, Holmen A. Fischer–Tropsch synthesis on monolithic catalysts with oil circulation. Catal Today 2005;105:357–61.
[117] Kapteijn F, Deugd RM, Moulijn JA. Fischer–Tropsch synthesis using monolithic catalysts. Catal Today 2005;105:350–6.
[118] Kizling MB, Jaras SG. A review of the use of plasma techniques in catalyst preparation and catalytic reactions. Appl Catal A: Gen 1996;147:1–21.
[119] Ishihara T, Eguchi K, Arai H. Hydrogenation of carbon monoxide over SiO_2-supported Fe–Co, Co–Ni and Ni–Fe bimetallic catalysts. Appl Catal 1987;30:225–38.
[120] Brumby A, Verhelst M, Cheret D. Recycling GTL catalysts – a new challenge. Catal Today 2005;106:166–9.
[121] Dunn BC, Covington DJ, Cole P, Pugmire RJ, Meuzelaar HLC, Ernst RD, Heider EC, Eyring EM. Silica xerogel supported cobalt metal Fischer – Tropsch catalysts for syngas to diesel range fuel conversion. Energy Fuels 2004;18:1519–21.
[122] Beretta A, Sun Q, Herman RG, Klier K. Production of methanol and isobutyl alcohol mixtures over double-bed cesium-promoted $Cu/ZnO/Cr_2O_3$ and ZnO/Cr_2O_3 catalysts. Ind Eng Chem Res 1996;35:1534–42.
[123] Epling W, Hoflund GB, Minahan DM. Reaction and surface characterization study of higher alcohol synthesis catalysts: VII. Cs- and Pd-promoted 1:1 Zn/Cr spinel. J Catal 1998;175:175–84.
[124] Hu J, Wang Y, Cao C, Elliott DC, Stevens DJ, White JF. Water gas shift reaction in a glass microreactor. Catal Today 2007;120:107–20.
[125] Sugier A, Freund EUS. Patent No. 4122110; October 1978.
[126] Sugier A, Freund EUS. Patent No. 4291126; September 1981.
[127] Kang S, Bae JW, Woo K, Sai-prasad PS, Jun K. ZSM-5 supported iron catalysts for Fischer–Tropsch production of light olefin. Fuel Process Technol 2010;91:399–403.
[128] Holy NL, Carey TF. Ethanol and n-propanol from syngas. Appl Catal 1985;19:219–23.
[129] Yu-Hua D, De-An C, Khi-Rui T. Promoter action of rare earth oxides in rhodium/silica catalysts for the conversion of syngas to ethanol. Appl Catal 1987;35:77–92.
[130] Gronchi P, Tempesti E, Mazzocchia C. Metal dispersion dependent selectivities for syngas conversion to ethanol on V_2O_3 supported rhodium. Appl Catal A: Gen 1994;120:115–26.
[131] Luo HY, Zhang W, Zhou HW, Huang SY, Lin PZ, Lin LW. A study of $Rh–Sm–V/SiO_2$ catalysts for the preparation of C_2-oxygenates from syngas. Appl Catal A: Gen 2001;214:161–6.
[132] Minahan DM, Epling WS, Hoflund GB. Reaction and surface characterization study of higher alcohol synthesis catalysts: IX. Pd- and alkali-promoted Zn/Cr-based spinels containing excess ZnO. J Catal 1998;179:241–57.
[133] Zaman SF, Smith KJ. Synthesis gas conversion over MoP catalysts. Catal Commun 2009;10:468–71.
[134] Mouaddib N, Perrichon V, Martin GA. Characterization of copper–cobalt catalysts for alcohol synthesis from syngas. Appl Catal A: Gen 1994;118:63–72.
[135] Zhang Y, Bao J, Nagamori S, Tsubaki N. A new and direct preparation method of iron-based bimodal catalyst and its application in Fischer–Tropsch synthesis. Appl Catal A: Gen 2009;352:277–81.
[136] Trepanier M, Dalai AK, Abatzoglou N. Synthesis of CNT-supported cobalt nanoparticle catalysts using a microemulsion technique: role of nanoparticle size on reducibility, activity and selectivity in Fischer–Tropsch reactions. Appl Catal A 2010;374:79–86.
[137] Vasireddy S, Campos A, Miamee E, Adeyiga A, Armstrong R, Allison JD, Spivey JJ. Study of attrition of Fe-based catalyst supported over spent FCC catalysts and their Fischer–Tropsch activity in a fixed bed reactor. Appl Catal A 2010;372:184–90.
[138] Song S, Lee S, Bae JW, Sai Prasad PS, Jun K, Shul Y. Effect of calcination temperature on the activity and cobalt crystallite size of Fischer–Tropsch $Co–Ru–Zr/SiO_2$ catalyst. Catal Lett 2009;129:233–9.
[139] Anon. Global energy perspectives to 2050 and beyond. Technical report. London: World Energy Council; 1995.
[140] Haber J, Block JH, Delmon B. Manual of methods and Procedures for catalyst characterization. Pure Appl Chem 1995;67:1257–306.
[141] Pant KK, Gupta RB. Fundamentals and use of hydrogen as fuel, hydrogen fuel production transport and storage. Florida, USA: Taylor and Francis Series; 2008.
[142] Gladden LF, Mantle MD, Sederman AJ. Magnetic resonance imaging of catalysts and catalytic processes. Adv Catal 2006;50:1–75.
[143] Pant KK, Gupta RB. Hydrogen storage in carbon materials, hydrogen fuel production transport and storage. Florida, USA: Taylor and Francis Series; 2008.
[144] Hagen J. Industrial catalysis a practical approach, Completely Revised and Extended Edition, Wiley-vch Verlag GmbH & Co. KGaA, Weinheim, Germany.
[145] Somorjai G.A., Li Y. Introduction to surface chemistry and catalysis, Second Edition, Wiley-vch Verlag GmbH & Co. KGaA, Weinheim, Germany.
[146] Tsuji J. Transition metal reagents and catalysts: innovations in organic synthesis. John Wiley & Sons, Ltd.; 2000; 1–477.
[147] Pant KK, Gupta RB. Hydrogen storage in metal hydrides, hydrogen fuel production transport and storage. Florida, USA: Taylor and Francis Series; 2008.
[148] Dincer I, Rosen MA. A worldwide perspective on energy, environment and sustainable development. Int J Energy Res 1998;22(15):1305–21.
[149] Dincer I. Renewable energy, environment and sustainable development. In: Proceedings of the world renewable energy congress. Florence, Italy; 20–25 September 1998. p. 2559–62.
[150] Rodrigues JJ, Fernandes FAN, Rodrigues MGF. Study of Co/SBA-15 catalysts prepared by microwave and conventional heating methods and application in Fischer–Tropsch synthesis. Appl Catal A: Gen 2013;468:32–7.
[151] Leonelli C, Mason TJ. Review – microwave and ultrasonic processing: now a realistic option for industry. Chem Eng Process 2010;49:885–900.
[152] Mohanty P, Pant KK, Parikh J, Sharma DK. Liquid fuel production from syngas using bifunctional $CuO–CoO–Cr_2O_3$ catalyst mixed with MFI zeolite. Fuel Process Technol 2011;92(3):600–8.
[153] Xiaofeng Z, Qingling C, Yuewu T, Huixin W. Influence of ultrasound impregnation on the performance of $Co/Zr/SiO_2$ catalyst during Fischer–Tropsch synthesis. Chin J Catal 2011;32(7):1156–65.
[154] Liang XY, Zhang LM, Ding HY, Qin YN. Supported catalyst $LaCoO_3/\gamma-Al_2O_3$ prepared by impregnating under ultrasound. Acta Phys – Chim Sin 2003;19(7):666–9.

[155] Pant KK, Mohanty P, Agarwal S, Dalai AK. Steam reforming of acetic acid for hydrogen production over bifunctional Ni–Co catalysts. Catal Today 2013;207:36–43.
[156] Fu T, Huang C, Lv J, Li Z. Fuel production through Fischer–Tropsch synthesis on carbon nanotubes supported Co catalyst prepared by plasma. Fuel 2014;121:225–31.
[157] Xiong H, Zhang Y, Wang S, Li J. Fischer–Tropsch synthesis: the effect of Al_2O_3 porosity on the performance of Co/Al_2O_3 catalyst. Catal Commun 2005;6:512–6.
[158] Mohanty P, Patel M, Pant KK. Hydrogen production from steam reforming of acetic acid over Cu–Zn supported calcium aluminate. Bioresour Technol 2012;123:558–65.
[159] Zou JJ, Zhang YP, Liu CJ. Reduction of supported noble-metal ions using glow discharge plasma. Langmuir 2006;22:11388–94.
[160] Mohanty P, Majhi S, Sahu JN, Pant KK. Response surface modeling and optimization of CO hydrogenation for higher liquid hydrocarbon using Cu–Co–Cr+ZSM-5 bifunctional catalyst. Ind Eng Chem Res 2012;51(13):4843–53.
[161] Liu CJ, Vissokov GP, Jang BWL. Catalyst preparation using plasma technologies. Catal Today 2002;72:173–84.
[162] Chu W, Wang LN, Chernavskii PA, KhodakovL AY. Glow-discharge plasmaassisted design of cobalt catalysts for Fischer–Tropsch synthesis. Angew Chem Int Ed 2008;47:5052–5.